American Diabetes Association. diabetes

Increase in Pancreatic Proinsulin and Preservation of Beta Cell Mass in Autoantibody Positive Donors prior to Type 1 Diabetes Onset

Journal:	*Diabetes*
Manuscript ID	DB16-1343.R2
Manuscript Type:	Original Article
Date Submitted by the Author:	n/a
Complete List of Authors:	Rodriguez-Calvo, Teresa; La Jolla Institute for Allergy and Immunology Zapardiel-Gonzalo, Jose; La Jolla Institute for Allergy and Immunology Amirian, Natalie; La Jolla Institute for Allergy and Immunology Castillo, Ericka; La Jolla Institute for Allergy and Immunology Lajevardi, Yasaman; La Jolla Institute for Allergy and Immunology Krogvold, Lars; Oslo university hospital, Division of Paediatric and Adolescent Medicine; Universitetet i Oslo Det medisinske fakultet Dahl-Jorgensen, Knut; Oslo Universitetssykehus, Division of Paediatric and Adolescent Medicine; Universitetet i Oslo Det medisinske fakultet von Herrath, Matthias; La Jolla Inst for Allergy & Immunol, Division of Developmental Immunology DI-3;

Increase in Pancreatic Proinsulin and Preservation of Beta Cell Mass in Autoantibody Positive Donors prior to Type 1 Diabetes Onset

Teresa Rodriguez-Calvo[1], Jose Zapardiel-Gonzalo[1], Natalie Amirian[1], Ericka Castillo[1], Yasaman Lajevardi[1], Lars Krogvold[3], Knut Dahl-Jørgensen[3] and Matthias G. von Herrath[1, 2].

[1]Type 1 Diabetes Center, La Jolla Institute for Allergy and Immunology, La Jolla, California, USA

[2]Novo Nordisk Diabetes Research & Development Center, Seattle, Washington, USA

[3]Division of Paediatric and Adolescent Medicine, Oslo University Hospital, Oslo, Norway and Faculty of Medicine, University of Oslo, Norway

Corresponding author: Matthias G. von Herrath; La Jolla Institute for Allergy and Immunology. 9420 Athena Circle, La Jolla, CA, 92037, USA. Phone: +1-858-205-0646. Fax: +1-858-752-6993. Email: matthias@lji.org; mtvh@novonordisk.com

Running Title: Increased proinsulin area in prediabetic donors

Word Count: 4428

Number of tables and figures: 1 table, 6 figures, 5 online supplementary figures, 1 online supplementary table.

Abbreviations:

Autoantibody positive: Ab+; proinsulin to C peptide ratio: PI/C; proinsulin area to insulin area ratio: PI/INS area ratio; Endoplasmic reticulum: ER

ABSTRACT

Type 1 diabetes is characterized by the loss of insulin production due to beta cell dysfunction and/or destruction. The hypothesis that beta cell loss occurs early during the pre-diabetic phase has recently been challenged. Here we show, for the first time *in situ* that in pancreas sections from autoantibody positive donors (Ab+) insulin area and beta cell mass are maintained prior to disease onset, and that production of proinsulin increases. This suggests that beta cell destruction occurs more precipitously than previously assumed. Indeed, the pancreatic proinsulin to insulin area ratio (PI /INS area ratio) was also increased in these prediabetic donors. Using high-resolution confocal microscopy we found a high accumulation of vesicles containing proinsulin in beta cells from Ab+ donors, suggesting either a defect in proinsulin conversion or an accumulation of immature vesicles due to an increase in insulin demand and/or to a dysfunction in vesicular trafficking. In addition, islets from Ab+ donors were larger and contained a higher number of beta cells per islet. Our data indicate that beta cell mass (and function) is maintained until shortly before diagnosis, and declines rapidly at the time of clinical onset of disease. This suggests that secondary prevention before onset, when beta cell mass is still intact, could be a successful therapeutic strategy.

Type 1 diabetes is defined as an autoimmune disease in which clinical symptoms arise as a result of beta cell loss. Genetic and environmental factors might render beta cells susceptible to attack by the immune system, or could contribute to beta cell dysfunction (1; 2). More than three decades ago, Eisenbarth described a linear loss of first phase insulin release following intravenous glucose administration in individuals with islet-cell antibodies who were followed for 10 years before diagnosis. However, elevations in fasting blood glucose and peak glucose during oral glucose tolerance tests were only seen in the year prior to onset (3). This sustained loss of beta cell function in prediabetic individuals strongly correlated with the time to overt diabetes and led to his landmark article in which the stages of type 1 diabetes were presented and where the steady decrease in insulin secretion was linked to a linear reduction in beta cell mass that continued after diagnosis (4). While this model remained a reference for many years, new studies have suggested that beta cell mass is not lost in a linear fashion during the prediabetic phase and a debate about the discrepancy between beta cell mass and function ensued (2). Subsequent studies have also detected a loss of glucose tolerance in the months preceding diagnosis (5; 6). Beta cell dysfunction might occur early in the disease process (at the point at which the individual becomes antibody positive), while an actual decline in beta cell mass might occur later. In the Diabetes Virus Detection (DiViD) study a transient beta cell dysfunction was detected in live cells obtained at diagnosis, which improved in a non-diabetic culture milieu (7). Increasing dysfunction would prompt an increase in insulin demand (8; 9), which could eventually cause a more cataclysmic decline in beta cell mass around the clinical onset of diabetes. However, the cause of the decline in function, and the precise time course of events have remained largely undefined.

Studies from the Network for Pancreatic Organ Donors with Diabetes (nPOD) have recently shown that beta cell mass is not diminished in Ab+ donors and that single beta cells and insulin containing islets can be found in donors with longstanding type 1 diabetes (10). The time course from seroconversion to onset of clinical diabetes has been further characterized in longitudinal studies. After autoantibody seroconversion, 14.5 % of single Ab+ and 67.9 % of multiple Ab+ patients progressed to type 1 diabetes in a 10-year follow-up study in 3 geographically different cohorts (11). In addition, it was also revealed that 11% of multiple Ab+ children would progress to clinical disease each year (12). However, the exact triggers and progression to clinical onset are not fully understood.

Proinsulin is an important autoantigen in type 1 diabetes in both humans and mice (13), as it shapes the autoreactive CD8 T cell repertoire (14; 15). Importantly, recent studies have shown that several epitopes within its precursor (preproinsulin) and proinsulin itself are recognized by islet infiltrating CD4 and/or CD8 T cells isolated from patients with type 1 diabetes (16-20), suggesting a potential role for this antigen in disease pathogenesis. Preproinsulin is processed into proinsulin and signal peptide (21). Only a marginal fraction of proinsulin is secreted to the circulation but it accounts for 30-50% of the protein production in beta cells and it increases in response to higher insulin demand. Because of this high metabolic demand, beta cells are prone to Endoplasmic Reticulum (ER) stress and proinsulin misfolding, which could lead to beta cell failure (22). ER stress may also be induced by viral infection (23), which was recently detected in the islets of Langerhans at diagnosis (24). Interestingly, it has been demonstrated that cytokine-induced ER stress enhances the exosomal release of proinsulin (25). Several reports present evidence of high

circulating proinsulin and proinsulin intermediates with or without accompanying hyperglycemia in patients at risk of developing the disease and after diagnosis (26; 27). Proinsulin and proinsulin to C-peptide ratios in combination with autoantibody concentration have been suggested as potential biomarkers for type 1 diabetes, capable of identifying with high sensitivity individuals at risk of developing disease one to forty months prior to clinical onset (28; 29). However, the link between proinsulin levels in serum and their content in the pancreas, in beta cells themselves, has not been investigated in human specimens *in situ*.

The objective of this study was to add refinement to the classical model of linear beta cell loss and to fill an important gap in our understanding of the prediabetic phase in human type 1 diabetes. We studied, for the first time in the human pancreas, the distribution of proinsulin in single and double Ab+ individuals, preceding the onset of disease as well as in recent-onset type 1 diabetes patients and correlated it with loss of insulin content, beta cell mass and proinsulin area to insulin area ratio (PI/INS area ratio). These studies underline the need for development of biomarkers as well as for preventive therapies focusing on normalizing beta cell dysfunction during the pre-diabetic stage.

RESEARCH DESIGN AND METHODS

Subjects

Human pancreas sections were collected from cadaveric organ donors through nPOD. Six µm sections from formalin-fixed paraffin-embedded (FFPE) sections from the head, body and tail of the pancreas were obtained from non-diabetic-single autoantibody positive (Ab+; n=8), non-diabetic double autoantibody positive (Ab+; n=5), non-diabetic

autoantibody negative controls (n=9) and one donor at onset of type 1 diabetes (n=1). In addition, four μm FFPE sections from living donors with type 1 diabetes (n=6) were obtained through the Diabetes Virus Detection (DiViD) study by tail resection (30). Overall, a total of 22 sections from head, 22 from body and 29 sections from the tail of the pancreas were analyzed (n=73 sections). Table 1 shows summarized demographic information for each group. Detailed donor information can be found in online supplementary table. All experimental procedures were approved by the La Jolla Institute for Allergy and Immunology Institutional Review Board-approved protocol number DI3-054-1112. For the DiViD study, participants provided written informed consent and more details can be found in (30).

Immunofluorescence

Pancreas sections were stained for insulin, proinsulin and glucagon following a standard triple indirect immunofluorescence (IF) staining. After deparaffinization and rehydration in descending ethanol concentrations, sections were exposed to heat-based antigen retrieval (citrate buffer). Staining was performed using a polyclonal guinea pig anti-insulin antibody (Dako, Carpinteria CA; 1:500), monoclonal mouse anti-proinsulin (DSHB clone GS-9A8 1:50) and monoclonal mouse anti-glucagon (Abcam; clone K79bB10, 1:300) conjugated in house to Alexa Fluor 647. Secondary antibodies included $F(ab')_2$ fragment of goat anti-guinea pig IgG conjugated to Alexa Fluor 488 (Jackson ImmunoResearch 1:800) and goat anti-mouse IgG (H+L) conjugated to Alexa Fluor 555 (Life Technologies, Grand Island NY; 1:1000) incubated at room temperature for 30 minutes. Sections were counterstained with Hoechst (Life Technologies; 1:400) for 10 minutes and then mounted with ProLong Gold anti-fade medium (Life technologies).

Image acquisition and analysis

All sections were scanned with an Axio Scan Z.1 slide scanner (Carl Zeiss microscopy, Thornwood, NY) using a fluorescent Orca Flash 4.0 v2 (HXP 120 V lamp) camera with a 20x/0.8NA objective for immunofluorescence. Images were acquired with ZEN2 software slidescan module. Acquisition settings were kept constant between specimens in order to allow for quantitative comparison between samples. ZEN2 software blue edition was used to process the images prior to analysis. Lower and upper thresholds were defined for each channel. For insulin and proinsulin, similar thresholds were set for comparison. Then whole tissue section images were exported and reduced at 30% or 45% depending on their size into .tiff files for automatic software analysis. Custom macros were developed to measure tissue area (macro #1), islet size and count (macro #2) and calculate the % of insulin, proinsulin and glucagon areas (macro #3; only cytoplasmic staining above background levels was measured). In order to classify and calculate the number of alpha and beta cells, the image of the whole tissue section was exported into 20x20 .tiff files in order to improve resolution, and then processed by a different custom macro (macro #4) (Supplementary Figure 1). All the macros were developed for Fiji (an image processing software developed for ImageJ, NIH). R software was used to systematically analyze the data (R is available as Free Software under the terms of the Free Software Foundation's GNU General Public License in source code form). In addition, three cases per group were analyzed by high-resolution confocal microscopy using an LSM 880 confocal microscope with Airyscan technology (Carl Zeiss, Jena, Germany) and a 63x objective.

Statistical analysis

Differences between group pairs were analyzed with a Student *t* test or Mann-Whitney test. Group differences were analyzed using one-way ANOVA follow by a Holm-Sidak multiple comparisons test or Kruskal Wallis follow by a Dunn multiple comparisons test. In order to assess the plausibility of using the ratio PI/INS area ratio as a discriminator for disease status, a logistic regression was fitted to the data using R version 3.3.0 (9).

A logistic regression (shown in figure 4C) was performed to assess the validity of the PI/INS area ratio as a risk classifier. The scores for this model were calculated as the distance from each point (plotted using their % of PI and INS area as coordinates) to the line PI = INS (i.e. y = x). Briefly: $score = \frac{Insulin - Proinsulin}{\sqrt{2}}$ The significance of the overall model was calculated by comparing it with a model with just the intercept (i.e. a null model). Besides the logistic regression, a Receiver Operating Characteristic (ROC) analysis using the R package ROCR version 1.0-7 (10) was performed to investigate the predictive power of the model.

Statistical analysis was performed using GraphPad Prism version 6 (GraphPad Software, San Diego California USA). Data in graphs and tables are presented as mean ± SD unless otherwise indicated. Findings were assumed statistically significant at $p \leq 0.05$.

RESULTS

Proinsulin area is significantly increased in autoantibody positive donor islets compared with non-diabetic controls while insulin area remains similar

We systematically measured insulin, proinsulin and glucagon staining from the head, body and tail regions of pancreatic tissue sections. Interestingly, there was a small increase in

total insulin area in Ab+ donors that did not reach statistical significance (Figure 1A, B, C, left panel). Conversely, a significant increase in proinsulin area was observed in head (54%, p=0.0233), body (57%, p=0.0143) and tail (60%, p=0.0087) regions in Ab+ individuals compared with control sections (Figure 1A, B, C, central panel). Lastly, there were no major differences in glucagon area between both groups for any of the regions (Figure 1A, B, C, right panel). To better understand whether this was due to a shift in the subcellular localization of proinsulin and/or to an increase in proinsulin content, a super high-resolution confocal microscope with Airyscan technology was used. In control donors, proinsulin was found to be mainly localized close to the nucleus with a staining pattern consistent with the Golgi apparatus and being minimally present in other compartments. In multiple Ab+ donors it was more widely localized to the juxtanuclear region (Golgi) and vesicular compartment, confirming a change in subcellular localization (Figure 2 and Supplementary Figure 2).

Beta cell mass is not reduced in single or double autoantibody positive donors

The combination of insulin area from the head, body and tail sections of the pancreas, normalized by the size of the respective tissues, was multiplied by the total weight of the pancreas. Mean beta cell mass was almost identical in controls and Ab+ donors (245.0 ± 60.5 mg controls vs 267.7 ± 80.2 mg Ab+, Figure 3A). However, when proinsulin area was used as reference instead of insulin, a significant increase in beta cell mass in the Ab+ donor group was seen (187.4 ± 49.7 mg controls vs 266.9 ± 99.7 mg Ab+, Figure 3B). Lastly, alpha cell mass, calculated as the adjusted percentage of glucagon area multiplied by the total weight of the pancreas, was similar for both, Ab+ and control groups (121.5 ± 42.6 mg controls vs 141.2 ± 65.7 mg Ab+, Figure 3C). Beta cell mass did not correlate with

age (r=-0.018; *p*=0.9341), BMI (r=0.377; *p*=0.0833) or time in intensive care unit (ICU) (r=-0.056; *p*=0.8250) (data not shown).

The proinsulin area to insulin area ratio is increased in autoantibody positive donors and constitutes a potential indicator of beta cell dysfunction.

In order to study the direct relation between insulin and proinsulin area in the pancreas, the PI/INS area ratio was calculated for each section, region and donor. Interestingly, the ratio was increased for Ab+ donors compared with controls for the head (38%; *p*=0.0031), body (40%; *p*=0.0005) and tail (32%; *p*=0.0004) regions of the pancreas (Figure 4A). To evaluate the use of the area ratio as a potential indicator of beta cell dysfunction and to directly compare Ab+ donors with controls, an arbitrary reference value of 1:1 (proinsulin area : insulin area) was chosen and graphically represented as a line to separate control from "at risk" donors. The distance from the donor's area values to the line was used as a score to estimate the risk of disease and to classify and distinguish control from Ab+ donors (Figure 4B). Then, a logistic regression was performed and the area under the curve (AUC) was calculated (Figure 4C). High AUC values, significant coefficients and a good model fit were obtained for head (AUC 0.85, coefficient *p*=0.0348, model *p*=0.00225), body (AUC 0.87, coefficient *p*=0.0213, model *p*=0.00073) and tail (AUC 0.9, coefficient *p*=0.0196, model *p*=0.00045), indicating that the pancreatic PI/INS area ratio could identify individuals at risk of developing disease.

In order to see if the insulin area, the proinsulin area, or the PI/INS area ratio could correlate with the risk of developing T1D, a "Risk Index" was calculated for all the donors based on their age, HLA and autoantibody status (Supplementary figure 3). To calculate the

Risk Index, a score of 0, 1 or 2 corresponding to low, medium or high risk was assigned as follows based on the risk of developing T1D: Age: >40 (0); 30-40 (1); 0-30 (2). HLA: No risk alleles (0); DR4 or DR3 only (1); DR4 DQ8 or DR3 DQ2 or DQ8 (2). Autoantibodies: 0 (0); 1 (1), 2 (2). The Risk Index was then calculated as the sum of the values obtained in each category for each donor (range 0 (minimum) to 6 (maximum)). There was a strong positive correlation between the risk index and the PI/INS area ratio (right panel) while there was a weak correlation with proinsulin area (central panel) and no correlation with insulin area (left panel) (Supplementary figure 3).

Patients with recent onset type 1 diabetes have more glucagon, less insulin and less proinsulin area but increased proinsulin to insulin area ratio.

To investigate the timing of the increase in proinsulin area and the inversion of the PI/INS area ratio when compared with control donors, pancreas tissue from a set of recently diagnosed patients with type 1 diabetes (0-9 weeks post-diagnosis) was studied (Figure 5). Only the tail region was analyzed, as all but one sample were obtained by tail resection as described in (30) (one section from a donor with type 1 diabetes at onset obtained from nPOD was also included for comparison). Patients with type 1 diabetes were compared to controls, and single and double Ab+ donors separately (Figure 5A). The insulin and proinsulin areas were lower than in the rest of the groups due to a reduction in the islets that contained insulin, whereas there was an increase in glucagon area (Figure 5C, 5D and 5F). Interestingly, the PI/INS area ratio was increased in patients with type 1 diabetes and almost identical to that of at risk, double Ab+ donors (0.77 ± 0.13 controls vs 0.99 ± 0.15 single Ab+ vs 1.06 ± 0.10 double Ab+ vs 1.07 ± 0.18 type 1 diabetes) (Figure 5E left panel).

Systematic analysis of islet size reveals heterogeneity within the pancreas and subtle differences between Ab+ donors and controls.

Small morphological alterations as well as in differences in islet number, size and distribution might occur many years before diagnosis, in individuals at risk of developing disease. First, the number of islets was counted and the total area of the tissue section was measured (see methods for details and Supplementary Figure 1). Total islet number and tissue size were variable across the pancreas but were similar in control and Ab+ donors (data not shown). There were no major differences in mean islet density between non-diabetic (head 2.5 ± 0.5 vs body 1.8 ± 0.2 vs tail 2.8 ± 0.7 islets/mm^2) and Ab+ donors (head 2.6 ± 0.7 vs body 2.1± 0.7 vs tail 3.1 ± 0.9 islets/mm^2) (Figure 6A). Next, the islet size distribution was analyzed. Significant differences were found between non-diabetic controls and double Ab+ donors for the head, body and tail (Figure 6B, Supplementary Figure 4). Lastly, sections from patients with type 1 diabetes were analyzed. Larger islets were found in these sections (Figure 5A and Supplementary Figure 4, tail region only), while the islet density was lower (Figure 5B), as expected. Interestingly, the tail of the pancreas presented a distinct islet distribution compared with the head and body regions for all groups, with a predominance of large islets and fewer small islets (Figure 6C, Supplementary Figure 4), confirming important regional differences within the pancreas.

Changes in the number of alpha and beta cells occur during the pre-diabetic phase and after onset of disease.

The number of insulin and glucagon expressing cells per islet was counted and the ratio between both cell populations was calculated (Supplementary Figure 5A). While no

significant differences were found, double Ab+ donors presented higher beta to alpha cell ratios in head, body and tail regions (Head median = 3.8 control vs 5.3 single Ab+ vs 6.4 double Ab+ / body median = 4.0 control vs 3.8 single Ab+ vs 7.1 double Ab+ / tail median = 3.6 control vs 3.8 single Ab+ vs 4.9 double Ab+). Amongst the Ab+ donors, very heterogeneous cell distribution patterns were found, with some individuals having a higher abundance of alpha cells per islet (Supplementary Figure 5B central panel) and others with a clear predominance of beta cells (Supplementary Figure 5B right panel) when compared with control sections (Supplementary Figure 5B left panel).

Patients with type 1 diabetes had a significantly lower beta to alpha cell ratio (median = 1.1 type 1 diabetes, tail region only) (Figure 5E right panel). Lastly, the percentage of islets containing only beta cells was calculated, which again, was similar for the control (24.9% ± 9.0), single (28.8% ± 9.9) and double Ab+ group (31.3% ± 16.8), and lower for the type 1 diabetes group (3.5% ± 4.9) (Figure 5G left panel). Islets with only alpha cells were not common (control 3.5% ± 3.2 vs single Ab+ 2.8% ± 0.8 vs double Ab+ 5.2% ±7.7). Only one double Ab+ donor (# 6267, 18.9%) and the donors with type 1 diabetes (52.2% ± 22.4) presented evident increases in the percentage of islets containing only alpha cells when compared with the rest of the donor groups (Figure 5G, right panel).

DISCUSSION

The recent access to human pancreata for research purposes and the subsequent histological studies have filled important gaps in our understanding of pancreatic pathology (10; 31-33). However, many fundamental questions remain to be answered. In this study, we aimed to fully characterize beta and alpha cells, investigating insulin, proinsulin and

glucagon content and distribution across head, body and tail regions of the human pancreas in healthy individuals and single as well as multiple Ab+ donors. In addition, we had access to a very unique subset of pancreatic tissues from living patients with recent-onset type 1 diabetes who participated in the DiViD study in which a small piece of the tail of the pancreas was surgically removed immediately in the months following diagnosis (30). Our study is the first to show an increase in pancreatic proinsulin area in prediabetic individuals and confirms the value of the PI/INS area ratio as an indicator of early beta cell dysfunction. In addition, we confirm previous findings that beta cell mass is not reduced in Ab+ individuals. We therefore add critical refinement to the original model of beta cell loss described by Eisenbarth three decades ago (4). We did not find any significant differences in the overall insulin positive area between healthy controls and Ab+ donors to support a reduction in insulin content long before the onset of disease. Moreover, beta cell mass was essentially identical in both groups, demonstrating that beta cells are preserved in Ab+ individuals until shortly before diagnosis and in agreement with previous publications that reported no differences in beta cell mass between non-diabetic and Ab+ donors (34-36).

Increases in proinsulin area were found in some of the single Ab+ pancreata, which could explain why the first phase insulin response is already abnormal in some of these individuals (4). Proinsulin primarily accumulates in the Golgi apparatus in resting beta cells and is further processed to insulin and C-peptide in immature secretory granules (37). Our data show~~s~~ significant increases in the proinsulin area in Ab+ individuals in the head, body and tail regions of the pancreas. Using a high-resolution confocal microscope to study a subset of samples, we observed that the increase in the proinsulin area was partially due to a shift in proinsulin subcellular localization, from the Golgi area in controls (juxta-nuclear)

to secretory vesicles in multiple Ab+ individuals (cytosolic). Although an increase in proinsulin area suggests an increase in the amount of proinsulin protein, additional experiments are needed to accurately measure the protein content. Nevertheless, this increase in area could be due to an increase in proinsulin production (to cover insulin demand), or to a defect in the processing and maturation of the existing pool of proinsulin to insulin, which is consequently released to the circulation. This is in agreement with studies which have detected proinsulinemia in prediabetic patients and patients with type 1 diabetes (38). In addition, an increase in proinsulin synthesis could lead to ER stress, protein misfolding and loss of glucose-stimulated insulin secretion (39). Other extrinsic factors, for example recurrent autoimmune attacks or other forms of metabolic stress (40; 41) may affect beta cell function and proinsulin processing early in the prediabetic disease process. In normal beta cells, up to 20% of proinsulin can be misfolded. However, only under pathological conditions and ER dysfunction, and once a certain level of misfolded proinsulin has been accumulated, beta cell toxicity and death can occur (22).

In a case-control study analysis by Sims and colleagues (42) an elevation of the proinsulin to C-peptide (PI/C) ratio preceded disease onset in high-risk subjects, and could be detected at least 12 months prior to diagnosis (42). This is in agreement with the data presented here, in which Ab+ individuals had an increase of the pancreatic PI/INS area ratio. Amongst the single Ab+ group, two donors (case 6170 and case 6184) consistently presented elevated PI/INS area ratio. This suggests that beta cells in these two individuals could have had a functional defect. Conversely, all but one double Ab+ donor (# 6080) presented an increased ratio in at least two of the three regions of the pancreas, supporting the notion of an early functional defect in beta cells during the prediabetic phase and prior

to diagnosis that does not necessarily imply beta cell loss. Donor 6080 was positive for Glutamic Acid Decarboxylase (GAD) and insulin autoantibodies but was 69 years old and therefore, unlikely to have developed the disease. In conclusion, our results, *in situ*, correlate well with those found in serum and confirm the potential of monitoring PI/C or PI/INS ratios as indicators of beta cell dysfunction.

The samples obtained from living individuals with recent-onset type 1 diabetes through the DiViD study (30) showed an expected significant decrease in the insulin and proinsulin area due to a reduced number of insulin-containing islets, however 4 out of 6 patients had elevated PI/INS area ratios suggesting that insulin therapy at onset might not fully alleviate the dysfunctional beta cells. Our findings indicate that potential therapies should target beta cells early before onset, when they still have the ability to be functionally rescued and when the immune system has not been fully activated.

We further characterized islet distribution and composition in order to study if small differences in islet pathology could be observed early in the prediabetic phase. The tail of the pancreas contained larger islets and higher islet density in all donor groups, which could point to important developmental and architectural differences in vascularization and innervation of the islets in this region (43; 44). Interestingly, subtle differences were found in double Ab+, at risk, individuals, in which larger islets were found in the body and tail region of the pancreas compared with controls. Moreover, this tendency was accentuated in recently diagnosed individuals with type 1 diabetes, where even larger islets could be found in the tail region, many of them containing only alpha cells. This is in agreement with previous studies in diabetic NOD mice in which small islets were preferentially lost and a

subsequent expansion of large islets was seen (45). An increase in the size of the islet and number of beta cells in multiple Ab+ donors could be a compensatory mechanism due to the chronic increase in insulin demand.

Our observations in the pancreas of individuals at risk of developing type 1 diabetes point to important and very early (at the first sign of autoimmunity) pathological changes in beta cells without an evident loss of beta cell mass. This confirms the potential benefit of estimating the PI/C or PI/INS ratios in Ab+ individuals in order to identify those patients at high risk at a stage where beta cells might still respond to preventive therapies and in order to enroll patients in clinical trials at a point in the disease when they would benefit the most. Whether a consequence of an increase in insulin demand, a primary cellular defect or a change in the orchestrated interplay between the immune system and the islet, the higher accumulation of proinsulin in beta cells without a reduction in insulin content might ultimately lead to beta cell exhaustion and death, with the subsequent release of beta cell antigens which initiate the autoimmune process. Whether type 1 diabetes is a primary autoimmune disease or autoimmunity is secondary to metabolic or functional defects that render beta cells susceptible to autoimmune destruction remains unknown. Future studies on proinsulin and insulin dynamics as well as a better characterization of beta cells themselves will provide the necessary answers to fully understand the pathological changes that precede the clinical onset of type 1 diabetes.

ACKNOWLEDGMENTS: This research was performed with the support of nPOD, a collaborative type 1 diabetes research project sponsored by the Juvenile Diabetes Research Foundation International (JDRF). Organ Procurement Organizations, partnering with nPOD to provide research resources, are listed at www.jdrfnpod.org/our-partners.php. The proinsulin antibody clone GS-9A8, developed by Madsen, O.D. was obtained from the Developmental Studies Hybridoma Bank, created by the NICHD of the NIH and maintained at The University of Iowa, Department of Biology, Iowa City, IA 52242. We would like to thank Zbigniew Mikulsky and Bill Kiosses of La Jolla Institute for Allergy and Immunology for their help with image acquisition and analysis, and Priscilla Colby of La Jolla Institute for Allergy and Immunology for administrative assistance

FUNDING: This study was supported by National Institutes of Health/National Institute of Allergy and Infectious Diseases Grant R01 AI092453-03.

DUALITY OF INTEREST: M.G.v.H. is an employee of Novo Nordisk. No other potential conflicts of interest relevant to this article were reported.

AUTHOR CONTRIBUTIONS: T.R-C. performed and designed experiments, analyzed and interpreted data, and wrote the manuscript. J.Z-G. designed the custom macros developed for computer assisted software analysis, analyzed and interpreted data using bioinformatics tools and helped with statistical analysis. N.A. performed experiments. E.C and Y.L helped with analysis. L.K, and K.D-J. collected patient material and revised the manuscript; K.D-J. is Principal Investigator of the DiViD study. M.v.H. designed experiments, interpreted data, and wrote the manuscript. M.v.H. is the guarantor of this work and, as such, had full access to all the data in the study and takes responsibility for the integrity of the data and the accuracy of the data analysis.

PRIOR PRESENTATION: Preliminary results from this study were presented at the Immunology of Diabetes Society 14th International Congress, Munich, Germany, 12-16 April 2015; the nPOD 8th Annual Scientific Meeting, Miami, FL, 22-25 February 2016; the 52nd Eruopean Association for the Study of Diabetes (EASD) Annual Meeting, Munich, Germany, 12-16 September 2016 and the 19th Inflammation Research Association (IRA)

International Meeting, San Diego, USA, 20-21 September 2016.

Tables

Table 1: Donor demographic information including age, percentage of males and females, ethnicity, BMI, disease duration and C-peptide levels.

	Control	Ab+	T1D	Total
n	9	13	7	29
Age (years) mean (±SD)	33.6 (±12.5)	36.1 (±13.5)	28.2 (±4.9)	32.6 (±4.1)
Female (%)	4 (44.5)	8 (61.5)	3 (42.8)	15 (51.7)
Male (%)	5 (55.5)	5 (38.5)	4 (57.2)	14 (48.3)
Ethnicity (%)				
African American	0 (0)	2 (15.4)	0 (0)	2 (6.9)
Caucasian	7 (77.7)	8 (61.5)	7 (100)	22 (75.9)
Hispanic	2 (22.3)	3 (23.1)	0 (0)	5 (17.2)
BMI mean (±SD)	28.2 (±6)	26.2 (±5)	25 (±3.2)	26.5 (±1.6)
Disease duration in weeks (±SD)			4.4 (±2.7)	
C-peptide (ng/ml) mean (±SD)	6.7 (±7.2)	6.1 (±6.2)	--------	

Figure legends:

Figure 1: *Proinsulin area but not insulin area is significantly increased in the pancreas of autoantibody positive donors compared with non-diabetic controls.* Insulin (left panel), proinsulin (middle panel) and glucagon (right panel) areas expressed as percentage of positive area were measured in whole tissue sections from the head **(A)**, body **(B)** and tail **(C)** region of the pancreas obtained from non-diabetic controls (n=9, black circles); single (n=8, black squares) and double (n=5, open squares) non-diabetic autoantibody positive cadaveric organ donors. * $p \leq 0.05$; ** $p \leq 0.01$.

Figure 2: *Proinsulin accumulates in the cytoplasmic compartment in beta cells from autoantibody positive donors.* Pancreatic sections from control (upper rows), single (middle rows) and double (lower rows) non-diabetic Ab+ cadaveric organ donors were stained for insulin (green), proinsulin (red), glucagon (white) and DAPI (blue) following a standard immunofluorescence staining protocol. The merged image can be seen on the right panel. Images were taken using a ZEISS LSM 880 confocal with Airyscan and a 63x objective. Scale bar 10µm.

Figure 3: *Beta cell mass is not reduced in single or double autoantibody positive donors*

A) Beta cell mass calculated as total pancreas weight multiplied by insulin area in non-diabetic controls, single and double non-diabetic autoantibody positive donors. **B)** Beta cell mass calculated as total pancreas weight multiplied by proinsulin area in non-diabetic controls, single and double non-diabetic autoantibody positive donors. **C)** Alpha cell mass calculated as total pancreas weight multiplied by glucagon area in non-diabetic controls, single and double non-diabetic autoantibody positive donors. All panels: Non-diabetic controls (n=9, black circles), single (n=8, black squares) and double (n=5, open squares) non-diabetic Ab+ cadaveric organ donors. * $p \leq 0.05$.

Figure 4: *The proinsulin to insulin area ratio is increased in autoantibody positive donors and constitutes a potential indicator of beta cell dysfunction.* **A)** The ratio between proinsulin and insulin area (PI/INS area ratio) was calculated for head (left panel), body (middle panel) and tail (right panel) regions of the pancreas from non-diabetic controls, single and double non-diabetic Ab+ donors. **B)** Proinsulin area versus insulin area XY plot: a theoretical reference value of 1:1

(proinsulin : insulin) was chosen and graphically represented as a line capable of separating control from "at risk" donors. The area under this line represents a ratio smaller than 1 and viceversa. The distance from the donor's area values to the line was used as a score to estimate the risk of developing disease and used to classify and distinguish control from Ab+ (single and double combined). **C)** Receiver Operating Characteristic (ROC) for the head (left panel), body (middle panel) and tail (right panel) regions of the pancreas; the Area Under the Curve (AUC) was calculated for the classifier described in B). The p-values show the significance of the logistic regression model including the predictor when compared to a model with just the intercept. Non-diabetic controls (n=9, black circles), single (n=8, black squares) and double (n=5, open squares) non-diabetic Ab+ cadaveric organ donors. ** $p \leq 0.01$; *** $p \leq 0.001$.

Figure 5: *Higher glucagon, lower insulin and proinsulin areas but increased proinsulin to insulin area ratio in recent onset type 1 diabetic patients.* **A)** Boxplots represent islet size distribution for non-diabetic controls (HC, n=5109), single (SingleAb, n=4692), double Ab+ (doubleAb, n=2859) and T1D (T1D, n=1748) donors in tail region of the pancreas. **B)** Islet density was calculated as the total number of islets per section divided by the total area of the tissue for the tail region of the pancreas. **C)** Representative image from whole tissue section of donor #6362, with type 1 diabetes, at onset. Insulin is shown in green, glucagon in red and DAPI in blue. Note the presence of insulin-deficient and insulin-containing islets scattered across the pancreas parenchyma. **D)** Insulin (left panel), proinsulin (middle panel) and glucagon (right panel) areas expressed as percentage of positive area were measured in whole tissue sections from the tail region of the pancreas. **E)** The proinsulin to insulin area ratio (PI/INS area ratio; left panel) and the beta to alpha cell ratio (right panel) were calculated for the pancreas tail region. **F)** Representative image of an islet from a recent-onset donor (DiViD study). Insulin is shown in green, proinsulin in red and glucagon in blue. **G)** The percentage of islets containing only beta cells (left panel) and only alpha cells (right panel) is shown. All panels: Non-diabetic controls (n=9, black circles), single (n=8, green squares), double (n=5, red squares) non-diabetic Ab+ and type 1 diabetes donors (n=7, blue triangles). * $p \leq 0.05$; ** $p \leq 0.01$; *** $p \leq 0.001$; **** $p \leq 0.0001$. Scale bar 500 μm in C) and 50 μm in F).

Figure 6: *Systematic analysis of islet distribution reveals heterogeneity within the pancreas and subtle differences between Ab+ donors and controls.* **A)** Islet density was calculated as the

total number of islets per section divided by the total area of the tissue for head, body and tail regions of the pancreas. Black circles represent control donors (n=9) while single Ab+ are shown in black squares (n=8) and double Ab+ in open squares (n=5). **B)** Boxplots represent islet size distribution for healthy controls, single and double Ab+ donors in head (left panel), body (middle panel) and tail (right panel) region of the pancreas. **C)** Boxplots represent islet size distribution for head, body and tail regions in healthy controls (left panel), single (middle panel) and double (right panel) Ab+. Number of islets: Head (HC n=4390; SingleAb n=4021, DoubleAb n=2067), body (HC n=3446; SingleAb n=4052, DoubleAb n=2043) and tail (HC n=5109; SingleAb n=4692, DoubleAb n=2859). * $p \leq 0.05$; ** $p \leq 0.01$; *** $p \leq 0.001$; **** $p \leq 0.0001$.

Supplementary Table 1: *Extended donor information*. Table S1 shows extended demographic and histological information, as well as the pancreatic regions analyzed for each donor. Autoab Pos, autoantibody positive donor. T1D, type 1 diabetic donor. Age and duration of disease are expressed in years unless otherwise indicated; BMI, body mass index; C-peptide is expressed in ng/ml; time ICU, time spent in the Intensive Care Unit (in days); ZnT8A, zinc transporter 8 autoantibodies; IA-2A, intracytoplasmic domain of the tyrosine phosphatase IA-2 autoantibodies; mIAA, micro assay for insulin autoantibodies; GADA, glutamic acid decarboxylase 65 autoantibodies. – Indicates not determined or not available.

Supplementary Figure 1: *Image acquisition and analysis.* All sections were scanned with an Axio Scan Z.1 slide scanner (Carl Zeiss microscopy, Thornwood, NY). A) For automated and systematic analysis, custom macros were developed to measure tissue area (macro #1, B middle panels); islet size and count (macro #2, B lower panels); calculate insulin, proinsulin and glucagon areas (macro #3, B upper panels). To classify and count alpha and beta cells, the image of the whole tissue section was exported into 20x20 smaller images in order to improve resolution, and then processed by a different custom macro (macro #4, C). Scale bar 500 μm in B and 50 μm in C.

Supplementary Figure 2: *Increase in proinsulin area and change in its subcellular localization without evident insulin depletion in autoantibody positive individuals.* High-resolution images and two-dimensional graphs of the intensities of pixels along the corresponding images from

control, single and double Ab+ donors. A column average plot is displayed representing the horizontal distance through the image (in µm) and the average pixel intensity for: A) proinsulin (red profile) and B) insulin (green profile). Scale bar 10 µm.

Supplementary figure 3: *Risk index*. Table: To calculate the Risk Index, a score of 0, 1 or 2 corresponding to low, medium or high risk was assigned as follows based on the risk of developing T1D: Age: >40 (0); 30-40 (1); 0-30 (2). HLA: No risk alleles (0); DR4 or DR3 only (1); DR4 DQ8 or DR3 DQ2 or DQ8 (2). Autoantibodies: 0 (0); 1 (1), 2 (2). The Risk Index was then calculated as the sum of the values obtained in each category for each donor (range 0 (minimum) to 6 (maximum)). Correlation analyses between the risk index and insulin area, proinsulin area and the PI/INS area ratio are shown for the head, body and tail regions (r and p-value area provided in the graph). Non-diabetic controls (n=9, black circles), single (n=8, green circles) and double (n=5, red circles) Ab+ cadaveric organ donors.

Supplementary Figure 4: *Increase in the size of the islets with autoantibody seroconversion and after onset of disease.* A) The median (table and bar graph) and interquantile range (IQR) of islet size distribution (μm^2) are shown for pancreas head, body and tail regions of control, single Ab+, double Ab+ and type 1 diabetes donors. Note the increase in islet size in double Ab+ and type 1 diabetes compared to controls.

Supplementary Figure 5: *Changes in the number of alpha and beta cells and their distribution in the islet can be observed during the pre-diabetic phase.* **A)** The number of alpha and beta cells per islet was counted and the ratio beta to alpha cell calculated for head (left panel), body (center panel) and tail (right panel) regions of the pancreas. Non-diabetic controls (n=9, black circles), single (n=8, green squares) and double (n=5, red squares) non-diabetic Ab+. **B)** Representative images from insulin (green), proinsulin (orange), glucagon (red) and DAPI (blue) staining on # 6102 control (left panel), # 6267 double Ab+ (center panel) and # 6158 double Ab+ (right panel). Note the different patterns of beta and alpha cell content as well as insulin, proinsulin and glucagon. A) normal pattern, B) predominantly alpha cells and C) predominantly beta cells. Scale bar 100 µm.

REFERENCES

1. Pugliese A: The multiple origins of Type 1 diabetes. Diabetic medicine : a journal of the British Diabetic Association 2013;30:135-146
2. van Belle TL, Coppieters KT, von Herrath MG: Type 1 diabetes: etiology, immunology, and therapeutic strategies. Physiological reviews 2011;91:79-118
3. Srikanta S, Ganda OP, Gleason RE, Jackson RA, Soeldner JS, Eisenbarth GS: Pre-type I diabetes. Linear loss of beta cell response to intravenous glucose. Diabetes 1984;33:717-720
4. Eisenbarth GS: Type I diabetes mellitus. A chronic autoimmune disease. The New England journal of medicine 1986;314:1360-1368
5. Sosenko JM, Skyler JS, Herold KC, Palmer JP, Type 1 Diabetes T, Diabetes Prevention Trial-Type 1 Study G: The metabolic progression to type 1 diabetes as indicated by serial oral glucose tolerance testing in the Diabetes Prevention Trial-type 1. Diabetes 2012;61:1331-1337
6. Helminen O, Aspholm S, Pokka T, Hautakangas MR, Haatanen N, Lempainen J, Ilonen J, Simell O, Knip M, Veijola R: HbA1c Predicts Time to Diagnosis of Type 1 Diabetes in Children at Risk. Diabetes 2015;64:1719-1727
7. Krogvold L, Skog O, Sundstrom G, Edwin B, Buanes T, Hanssen KF, Ludvigsson J, Grabherr M, Korsgren O, Dahl-Jorgensen K: Function of Isolated Pancreatic Islets From Patients at Onset of Type 1 Diabetes: Insulin Secretion Can Be Restored After Some Days in a Nondiabetogenic Environment In Vitro: Results From the DiViD Study. Diabetes 2015;64:2506-2512
8. Marre ML, James EA, Piganelli JD: beta cell ER stress and the implications for immunogenicity in type 1 diabetes. Frontiers in cell and developmental biology 2015;3:67
9. Eizirik DL, Cnop M: ER stress in pancreatic beta cells: the thin red line between adaptation and failure. Science signaling 2010;3:pe7
10. Campbell-Thompson M, Fu A, Kaddis JS, Wasserfall C, Schatz DA, Pugliese A, Atkinson MA: Insulitis and beta-Cell Mass in the Natural History of Type 1 Diabetes. Diabetes 2016;65:719-731
11. Ziegler AG, Rewers M, Simell O, Simell T, Lempainen J, Steck A, Winkler C, Ilonen J, Veijola R, Knip M, Bonifacio E, Eisenbarth GS: Seroconversion to multiple islet autoantibodies and risk of progression to diabetes in children. Jama 2013;309:2473-2479
12. Bonifacio E: Predicting type 1 diabetes using biomarkers. Diabetes care 2015;38:989-996
13. Narendran P, Mannering SI, Harrison LC: Proinsulin-a pathogenic autoantigen in type 1 diabetes. Autoimmunity reviews 2003;2:204-210
14. Thayer TC, Pearson JA, De Leenheer E, Hanna SJ, Boldison J, Davies J, Tsui A, Ahmed S, Easton P, Siew LK, Wen L, Wong FS: Peripheral Proinsulin Expression Controls Low-Avidity Proinsulin-Reactive CD8 T Cells in Type 1 Diabetes. Diabetes 2016;65:3429-3439
15. Pearson JA, Thayer TC, McLaren JE, Ladell K, De Leenheer E, Phillips A, Davies J, Kakabadse D, Miners K, Morgan P, Wen L, Price DA, Wong FS: Proinsulin Expression Shapes the TCR Repertoire but Fails to Control the Development of Low-Avidity Insulin-Reactive CD8+ T Cells. Diabetes 2016;65:1679-1689
16. Toma A, Laika T, Haddouk S, Luce S, Briand JP, Camoin L, Connan F, Lambert M, Caillat-Zucman S, Carel JC, Muller S, Choppin J, Lemonnier F, Boitard C: Recognition of human proinsulin leader sequence by class I-restricted T-cells in HLA-A*0201 transgenic mice and in human type 1 diabetes. Diabetes 2009;58:394-402
17. Toma A, Haddouk S, Briand JP, Camoin L, Gahery H, Connan F, Dubois-Laforgue D, Caillat-Zucman S, Guillet JG, Carel JC, Muller S, Choppin J, Boitard C: Recognition of a

subregion of human proinsulin by class I-restricted T cells in type 1 diabetic patients. Proceedings of the National Academy of Sciences of the United States of America 2005;102:10581-10586
18. Mallone R, Martinuzzi E, Blancou P, Novelli G, Afonso G, Dolz M, Bruno G, Chaillous L, Chatenoud L, Bach JM, van Endert P: CD8+ T-cell responses identify beta-cell autoimmunity in human type 1 diabetes. Diabetes 2007;56:613-621
19. Michels AW, Landry LG, McDaniel KA, Yu L, Campbell-Thompson M, Kwok WW, Jones KL, Gottlieb PA, Kappler JW, Tang Q, Roep BO, Atkinson MA, Mathews CE, Nakayama M: Islet-derived CD4 T-cells targeting proinsulin in human autoimmune diabetes. Diabetes 2016;
20. Babon JA, DeNicola ME, Blodgett DM, Crevecoeur I, Buttrick TS, Maehr R, Bottino R, Naji A, Kaddis J, Elyaman W, James EA, Haliyur R, Brissova M, Overbergh L, Mathieu C, Delong T, Haskins K, Pugliese A, Campbell-Thompson M, Mathews C, Atkinson MA, Powers AC, Harlan DM, Kent SC: Analysis of self-antigen specificity of islet-infiltrating T cells from human donors with type 1 diabetes. Nature medicine 2016;22:1482-1487
21. Liu M, Wright J, Guo H, Xiong Y, Arvan P: Proinsulin entry and transit through the endoplasmic reticulum in pancreatic beta cells. Vitamins and hormones 2014;95:35-62
22. Sun J, Cui J, He Q, Chen Z, Arvan P, Liu M: Proinsulin misfolding and endoplasmic reticulum stress during the development and progression of diabetes. Molecular aspects of medicine 2015;42:105-118
23. de Beeck AO, Eizirik DL: Viral infections in type 1 diabetes mellitus--why the beta cells? Nature reviews Endocrinology 2016;12:263-273
24. Krogvold L, Edwin B, Buanes T, Frisk G, Skog O, Anagandula M, Korsgren O, Undlien D, Eike MC, Richardson SJ, Leete P, Morgan NG, Oikarinen S, Oikarinen M, Laiho JE, Hyoty H, Ludvigsson J, Hanssen KF, Dahl-Jorgensen K: Detection of a low-grade enteroviral infection in the islets of langerhans of living patients newly diagnosed with type 1 diabetes. Diabetes 2015;64:1682-1687
25. Cianciaruso C, Phelps EA, Pasquier M, Hamelin R, Demurtas D, Ahmed MA, Piemonti L, Hirosue S, Swartz MA, De Palma M, Hubbell JA, Baekkeskov S: Primary Human and Rat Beta Cells Release the Intracellular Autoantigens GAD65, IA-2 and Proinsulin in Exosomes Together with Cytokine-Induced Enhancers of Immunity. Diabetes 2016;
26. Roder ME, Knip M, Hartling SG, Karjalainen J, Akerblom HK, Binder C: Disproportionately elevated proinsulin levels precede the onset of insulin-dependent diabetes mellitus in siblings with low first phase insulin responses. The Childhood Diabetes in Finland Study Group. The Journal of clinical endocrinology and metabolism 1994;79:1570-1575
27. Hartling SG, Knip M, Roder ME, Dinesen B, Akerblom HK, Binder C: Longitudinal study of fasting proinsulin in 148 siblings of patients with insulin-dependent diabetes mellitus. Study Group on Childhood Diabetes in Finland. European journal of endocrinology / European Federation of Endocrine Societies 1997;137:490-494
28. Truyen I, De Pauw P, Jorgensen PN, Van Schravendijk C, Ubani O, Decochez K, Vandemeulebroucke E, Weets I, Mao R, Pipeleers DG, Gorus FK, Belgian Diabetes R: Proinsulin levels and the proinsulin:c-peptide ratio complement autoantibody measurement for predicting type 1 diabetes. Diabetologia 2005;48:2322-2329
29. Watkins RA, Evans-Molina C, Terrell JK, Day KH, Guindon L, Restrepo IA, Mirmira RG, Blum JS, DiMeglio LA: Proinsulin and heat shock protein 90 as biomarkers of beta-cell stress in the early period after onset of type 1 diabetes. Translational research : the journal of laboratory and clinical medicine 2016;168:96-106 e101

30. Krogvold L, Edwin B, Buanes T, Ludvigsson J, Korsgren O, Hyoty H, Frisk G, Hanssen KF, Dahl-Jorgensen K: Pancreatic biopsy by minimal tail resection in live adult patients at the onset of type 1 diabetes: experiences from the DiViD study. Diabetologia 2014;57:841-843
31. Kaddis JS, Pugliese A, Atkinson MA: A run on the biobank: what have we learned about type 1 diabetes from the nPOD tissue repository? Current opinion in endocrinology, diabetes, and obesity 2015;22:290-295
32. Pugliese A, Vendrame F, Reijonen H, Atkinson MA, Campbell-Thompson M, Burke GW: New insight on human type 1 diabetes biology: nPOD and nPOD-transplantation. Current diabetes reports 2014;14:530
33. Campbell-Thompson M: Organ donor specimens: What can they tell us about type 1 diabetes? Pediatric diabetes 2015;16:320-330
34. Wagner R, McNally JM, Bonifacio E, Genovese S, Foulis A, McGill M, Christie MR, Betterle C, Bosi E, Bottazzo GF: Lack of immunohistological changes in the islets of nondiabetic, autoimmune, polyendocrine patients with beta-selective GAD-specific islet cell antibodies. Diabetes 1994;43:851-856
35. In't Veld P, Lievens D, De Grijse J, Ling Z, Van der Auwera B, Pipeleers-Marichal M, Gorus F, Pipeleers D: Screening for insulitis in adult autoantibody-positive organ donors. Diabetes 2007;56:2400-2404
36. Diedisheim M, Mallone R, Boitard C, Larger E: beta-cell Mass in Nondiabetic Autoantibody-Positive Subjects: An Analysis Based on the Network for Pancreatic Organ Donors Database. The Journal of clinical endocrinology and metabolism 2016;101:1390-1397
37. Haataja L, Snapp E, Wright J, Liu M, Hardy AB, Wheeler MB, Markwardt ML, Rizzo M, Arvan P: Proinsulin intermolecular interactions during secretory trafficking in pancreatic beta cells. The Journal of biological chemistry 2013;288:1896-1906
38. Hostens K, Ling Z, Van Schravendijk C, Pipeleers D: Prolonged exposure of human beta-cells to high glucose increases their release of proinsulin during acute stimulation with glucose or arginine. The Journal of clinical endocrinology and metabolism 1999;84:1386-1390
39. Wang S, Kaufman RJ: The impact of the unfolded protein response on human disease. The Journal of cell biology 2012;197:857-867
40. Oresic M, Simell S, Sysi-Aho M, Nanto-Salonen K, Seppanen-Laakso T, Parikka V, Katajamaa M, Hekkala A, Mattila I, Keskinen P, Yetukuri L, Reinikainen A, Lahde J, Suortti T, Hakalax J, Simell T, Hyoty H, Veijola R, Ilonen J, Lahesmaa R, Knip M, Simell O: Dysregulation of lipid and amino acid metabolism precedes islet autoimmunity in children who later progress to type 1 diabetes. The Journal of experimental medicine 2008;205:2975-2984
41. Sysi-Aho M, Ermolov A, Gopalacharyulu PV, Tripathi A, Seppanen-Laakso T, Maukonen J, Mattila I, Ruohonen ST, Vahatalo L, Yetukuri L, Harkonen T, Lindfors E, Nikkila J, Ilonen J, Simell O, Saarela M, Knip M, Kaski S, Savontaus E, Oresic M: Metabolic regulation in progression to autoimmune diabetes. PLoS computational biology 2011;7:e1002257
42. Sims EK, Chaudhry Z, Watkins R, Syed F, Blum J, Ouyang F, Perkins SM, Mirmira RG, Sosenko J, DiMeglio LA, Evans-Molina C: Elevations in the Fasting Serum Proinsulin-to-C-Peptide Ratio Precede the Onset of Type 1 Diabetes. Diabetes care 2016;
43. Amella C, Cappello F, Kahl P, Fritsch H, Lozanoff S, Sergi C: Spatial and temporal dynamics of innervation during the development of fetal human pancreas. Neuroscience 2008;154:1477-1487
44. Lammert E, Cleaver O, Melton D: Induction of pancreatic differentiation by signals from blood vessels. Science 2001;294:564-567

45. Alanentalo T, Hornblad A, Mayans S, Karin Nilsson A, Sharpe J, Larefalk A, Ahlgren U, Holmberg D: Quantification and three-dimensional imaging of the insulitis-induced destruction of beta-cells in murine type 1 diabetes. Diabetes 2010;59:1756-1764

Increase in Pancreatic Proinsulin and Preservation of Beta Cell Mass in Autoantibody Positive Donors prior to Type 1 Diabetes Onset

Teresa Rodriguez-Calvo[1], Jose Zapardiel-Gonzalo[1], Natalie Amirian[1], Ericka Castillo[1], Yasaman Lajevardi[1], Lars Krogvold[3], Knut Dahl-Jørgensen[3] and Matthias G. von Herrath[1, 2].

[1]Type 1 Diabetes Center, La Jolla Institute for Allergy and Immunology, La Jolla, California, USA

[2]Novo Nordisk Diabetes Research & Development Center, Seattle, Washington, USA

[3]Division of Paediatric and Adolescent Medicine, Oslo University Hospital, Oslo, Norway and Faculty of Medicine, University of Oslo, Norway

Corresponding author: Matthias G. von Herrath; La Jolla Institute for Allergy and Immunology. 9420 Athena Circle, La Jolla, CA, 92037, USA. Phone: +1-858-205-0646. Fax: +1-858-752-6993. Email: matthias@lji.org; mtvh@novonordisk.com

Running Title: Increased proinsulin area in prediabetic donors

Word Count: 4428

Number of tables and figures: 1 table, 6 figures, 5 online supplementary figures, 1 online supplementary table.

Abbreviations:

Autoantibody positive: Ab+; proinsulin to C peptide ratio: PI/C; proinsulin area to insulin area ratio: PI/INS area ratio; Endoplasmic reticulum: ER

ABSTRACT

Type 1 diabetes is characterized by the loss of insulin production due to beta cell dysfunction and/or destruction. The hypothesis that beta cell loss occurs early during the pre-diabetic phase has recently been challenged. Here we show, for the first time *in situ* that in pancreas sections from autoantibody positive donors (Ab+) insulin area and beta cell mass are maintained prior to disease onset, and that production of proinsulin increases. This suggests that beta cell destruction occurs more precipitously than previously assumed. Indeed, the pancreatic proinsulin to insulin area ratio (PI /INS area ratio) was also increased in these prediabetic donors. Using high-resolution confocal microscopy we found a high accumulation of vesicles containing proinsulin in beta cells from Ab+ donors, suggesting either a defect in proinsulin conversion or an accumulation of immature vesicles due to an increase in insulin demand and/or to a dysfunction in vesicular trafficking. In addition, islets from Ab+ donors were larger and contained a higher number of beta cells per islet. Our data indicate that beta cell mass (and function) is maintained until shortly before diagnosis, and declines rapidly at the time of clinical onset of disease. This suggests that secondary prevention before onset, when beta cell mass is still intact, could be a successful therapeutic strategy.

Type 1 diabetes is defined as an autoimmune disease in which clinical symptoms arise as a result of beta cell loss. Genetic and environmental factors might render beta cells susceptible to attack by the immune system, or could contribute to beta cell dysfunction (1; 2). More than three decades ago, Eisenbarth described a linear loss of first phase insulin release following intravenous glucose administration in individuals with islet-cell antibodies who were followed for 10 years before diagnosis. However, elevations in fasting blood glucose and peak glucose during oral glucose tolerance tests were only seen in the year prior to onset (3). This sustained loss of beta cell function in prediabetic individuals strongly correlated with the time to overt diabetes and led to his landmark article in which the stages of type 1 diabetes were presented and where the steady decrease in insulin secretion was linked to a linear reduction in beta cell mass that continued after diagnosis (4). While this model remained a reference for many years, new studies have suggested that beta cell mass is not lost in a linear fashion during the prediabetic phase and a debate about the discrepancy between beta cell mass and function ensued (2). Subsequent studies have also detected a loss of glucose tolerance in the months preceding diagnosis (5; 6). Beta cell dysfunction might occur early in the disease process (at the point at which the individual becomes antibody positive), while an actual decline in beta cell mass might occur later. In the Diabetes Virus Detection (DiViD) study a transient beta cell dysfunction was detected in live cells obtained at diagnosis, which improved in a non-diabetic culture milieu (7). Increasing dysfunction would prompt an increase in insulin demand (8; 9), which could eventually cause a more cataclysmic decline in beta cell mass around the clinical onset of diabetes. However, the cause of the decline in function, and the precise time course of events have remained largely undefined.

Studies from the Network for Pancreatic Organ Donors with Diabetes (nPOD) have recently shown that beta cell mass is not diminished in Ab+ donors and that single beta cells and insulin containing islets can be found in donors with longstanding type 1 diabetes (10). The time course from seroconversion to onset of clinical diabetes has been further characterized in longitudinal studies. After autoantibody seroconversion, 14.5 % of single Ab+ and 67.9 % of multiple Ab+ patients progressed to type 1 diabetes in a 10-year follow-up study in 3 geographically different cohorts (11). In addition, it was also revealed that 11% of multiple Ab+ children would progress to clinical disease each year (12). However, the exact triggers and progression to clinical onset are not fully understood.

Proinsulin is an important autoantigen in type 1 diabetes in both humans and mice (13), as it shapes the autoreactive CD8 T cell repertoire (14; 15). Importantly, recent studies have shown that several epitopes within its precursor (preproinsulin) and proinsulin itself are recognized by islet infiltrating CD4 and/or CD8 T cells isolated from patients with type 1 diabetes (16-20), suggesting a potential role for this antigen in disease pathogenesis. Preproinsulin is processed into proinsulin and signal peptide (21). Only a marginal fraction of proinsulin is secreted to the circulation but it accounts for 30-50% of the protein production in beta cells and it increases in response to higher insulin demand. Because of this high metabolic demand, beta cells are prone to Endoplasmic Reticulum (ER) stress and proinsulin misfolding, which could lead to beta cell failure (22). ER stress may also be induced by viral infection (23), which was recently detected in the islets of Langerhans at diagnosis (24). Interestingly, it has been demonstrated that cytokine-induced ER stress enhances the exosomal release of proinsulin (25). Several reports present evidence of high

circulating proinsulin and proinsulin intermediates with or without accompanying hyperglycemia in patients at risk of developing the disease and after diagnosis (26; 27). Proinsulin and proinsulin to C-peptide ratios in combination with autoantibody concentration have been suggested as potential biomarkers for type 1 diabetes, capable of identifying with high sensitivity individuals at risk of developing disease one to forty months prior to clinical onset (28; 29). However, the link between proinsulin levels in serum and their content in the pancreas, in beta cells themselves, has not been investigated in human specimens *in situ*.

The objective of this study was to add refinement to the classical model of linear beta cell loss and to fill an important gap in our understanding of the prediabetic phase in human type 1 diabetes. We studied, for the first time in the human pancreas, the distribution of proinsulin in single and double Ab+ individuals, preceding the onset of disease as well as in recent-onset type 1 diabetes patients and correlated it with loss of insulin content, beta cell mass and proinsulin area to insulin area ratio (PI/INS area ratio). These studies underline the need for development of biomarkers as well as for preventive therapies focusing on normalizing beta cell dysfunction during the pre-diabetic stage.

RESEARCH DESIGN AND METHODS

Subjects

Human pancreas sections were collected from cadaveric organ donors through nPOD. Six µm sections from formalin-fixed paraffin-embedded (FFPE) sections from the head, body and tail of the pancreas were obtained from non-diabetic-single autoantibody positive (Ab+; n=8), non-diabetic double autoantibody positive (Ab+; n=5), non-diabetic

autoantibody negative controls (n=9) and one donor at onset of type 1 diabetes (n=1). In addition, four μm FFPE sections from living donors with type 1 diabetes (n=6) were obtained through the Diabetes Virus Detection (DiViD) study by tail resection (30). Overall, a total of 22 sections from head, 22 from body and 29 sections from the tail of the pancreas were analyzed (n=73 sections). Table 1 shows summarized demographic information for each group. Detailed donor information can be found in online supplementary table. All experimental procedures were approved by the La Jolla Institute for Allergy and Immunology Institutional Review Board-approved protocol number DI3-054-1112. For the DiViD study, participants provided written informed consent and more details can be found in (30).

Immunofluorescence

Pancreas sections were stained for insulin, proinsulin and glucagon following a standard triple indirect immunofluorescence (IF) staining. After deparaffinization and rehydration in descending ethanol concentrations, sections were exposed to heat-based antigen retrieval (citrate buffer). Staining was performed using a polyclonal guinea pig anti-insulin antibody (Dako, Carpinteria CA; 1:500), monoclonal mouse anti-proinsulin (DSHB clone GS-9A8 1:50) and monoclonal mouse anti-glucagon (Abcam; clone K79bB10, 1:300) conjugated in house to Alexa Fluor 647. Secondary antibodies included $F(ab')_2$ fragment of goat anti-guinea pig IgG conjugated to Alexa Fluor 488 (Jackson ImmunoResearch 1:800) and goat anti-mouse IgG (H+L) conjugated to Alexa Fluor 555 (Life Technologies, Grand Island NY; 1:1000) incubated at room temperature for 30 minutes. Sections were counterstained with Hoechst (Life Technologies; 1:400) for 10 minutes and then mounted with ProLong Gold anti-fade medium (Life technologies).

Image acquisition and analysis

All sections were scanned with an Axio Scan Z.1 slide scanner (Carl Zeiss microscopy, Thornwood, NY) using a fluorescent Orca Flash 4.0 v2 (HXP 120 V lamp) camera with a 20x/0.8NA objective for immunofluorescence. Images were acquired with ZEN2 software slidescan module. Acquisition settings were kept constant between specimens in order to allow for quantitative comparison between samples. ZEN2 software blue edition was used to process the images prior to analysis. Lower and upper thresholds were defined for each channel. For insulin and proinsulin, similar thresholds were set for comparison. Then whole tissue section images were exported and reduced at 30% or 45% depending on their size into .tiff files for automatic software analysis. Custom macros were developed to measure tissue area (macro #1), islet size and count (macro #2) and calculate the % of insulin, proinsulin and glucagon areas (macro #3; only cytoplasmic staining above background levels was measured). In order to classify and calculate the number of alpha and beta cells, the image of the whole tissue section was exported into 20x20 .tiff files in order to improve resolution, and then processed by a different custom macro (macro #4) (Supplementary Figure 1). All the macros were developed for Fiji (an image processing software developed for ImageJ, NIH). R software was used to systematically analyze the data (R is available as Free Software under the terms of the Free Software Foundation's GNU General Public License in source code form). In addition, three cases per group were analyzed by high-resolution confocal microscopy using an LSM 880 confocal microscope with Airyscan technology (Carl Zeiss, Jena, Germany) and a 63x objective.

Statistical analysis

Differences between group pairs were analyzed with a Student *t* test or Mann-Whitney test. Group differences were analyzed using one-way ANOVA follow by a Holm-Sidak multiple comparisons test or Kruskal Wallis follow by a Dunn multiple comparisons test. In order to assess the plausibility of using the ratio PI/INS area ratio as a discriminator for disease status, a logistic regression was fitted to the data using R version 3.3.0 (9).

A logistic regression (shown in figure 4C) was performed to assess the validity of the PI/INS area ratio as a risk classifier. The scores for this model were calculated as the distance from each point (plotted using their % of PI and INS area as coordinates) to the line PI = INS (i.e. y = x). Briefly: $score = \frac{Insulin - Proinsulin}{\sqrt{2}}$ The significance of the overall model was calculated by comparing it with a model with just the intercept (i.e. a null model). Besides the logistic regression, a Receiver Operating Characteristic (ROC) analysis using the R package ROCR version 1.0-7 (10) was performed to investigate the predictive power of the model.

Statistical analysis was performed using GraphPad Prism version 6 (GraphPad Software, San Diego California USA). Data in graphs and tables are presented as mean ± SD unless otherwise indicated. Findings were assumed statistically significant at $p \leq 0.05$.

RESULTS

Proinsulin area is significantly increased in autoantibody positive donor islets compared with non-diabetic controls while insulin area remains similar

We systematically measured insulin, proinsulin and glucagon staining from the head, body and tail regions of pancreatic tissue sections. Interestingly, there was a small increase in

total insulin area in Ab+ donors that did not reach statistical significance (Figure 1A, B, C, left panel). Conversely, a significant increase in proinsulin area was observed in head (54%, p=0.0233), body (57%, p=0.0143) and tail (60%, p=0.0087) regions in Ab+ individuals compared with control sections (Figure 1A, B, C, central panel). Lastly, there were no major differences in glucagon area between both groups for any of the regions (Figure 1A, B, C, right panel). To better understand whether this was due to a shift in the subcellular localization of proinsulin and/or to an increase in proinsulin content, a super high-resolution confocal microscope with Airyscan technology was used. In control donors, proinsulin was found to be mainly localized close to the nucleus with a staining pattern consistent with the Golgi apparatus and being minimally present in other compartments. In multiple Ab+ donors it was more widely localized to the juxtanuclear region (Golgi) and vesicular compartment, confirming a change in subcellular localization (Figure 2 and Supplementary Figure 2).

Beta cell mass is not reduced in single or double autoantibody positive donors

The combination of insulin area from the head, body and tail sections of the pancreas, normalized by the size of the respective tissues, was multiplied by the total weight of the pancreas. Mean beta cell mass was almost identical in controls and Ab+ donors (245.0 ± 60.5 mg controls vs 267.7 ± 80.2 mg Ab+, Figure 3A). However, when proinsulin area was used as reference instead of insulin, a significant increase in beta cell mass in the Ab+ donor group was seen (187.4 ± 49.7 mg controls vs 266.9 ± 99.7 mg Ab+, Figure 3B). Lastly, alpha cell mass, calculated as the adjusted percentage of glucagon area multiplied by the total weight of the pancreas, was similar for both, Ab+ and control groups (121.5 ± 42.6 mg controls vs 141.2 ± 65.7 mg Ab+, Figure 3C). Beta cell mass did not correlate with

age (r=-0.018; *p*=0.9341), BMI (r=0.377; *p*=0.0833) or time in intensive care unit (ICU) (r=-0.056; *p*=0.8250) (data not shown).

The proinsulin area to insulin area ratio is increased in autoantibody positive donors and constitutes a potential indicator of beta cell dysfunction.

In order to study the direct relation between insulin and proinsulin area in the pancreas, the PI/INS area ratio was calculated for each section, region and donor. Interestingly, the ratio was increased for Ab+ donors compared with controls for the head (38%; *p*=0.0031), body (40%; *p*=0.0005) and tail (32%; *p*=0.0004) regions of the pancreas (Figure 4A). To evaluate the use of the area ratio as a potential indicator of beta cell dysfunction and to directly compare Ab+ donors with controls, an arbitrary reference value of 1:1 (proinsulin area : insulin area) was chosen and graphically represented as a line to separate control from "at risk" donors. The distance from the donor's area values to the line was used as a score to estimate the risk of disease and to classify and distinguish control from Ab+ donors (Figure 4B). Then, a logistic regression was performed and the area under the curve (AUC) was calculated (Figure 4C). High AUC values, significant coefficients and a good model fit were obtained for head (AUC 0.85, coefficient *p*=0.0348, model *p*=0.00225), body (AUC 0.87, coefficient *p*=0.0213, model *p*=0.00073) and tail (AUC 0.9, coefficient *p*=0.0196, model *p*=0.00045), indicating that the pancreatic PI/INS area ratio could identify individuals at risk of developing disease.

In order to see if the insulin area, the proinsulin area, or the PI/INS area ratio could correlate with the risk of developing T1D, a "Risk Index" was calculated for all the donors based on their age, HLA and autoantibody status (Supplementary figure 3). To calculate the

Risk Index, a score of 0, 1 or 2 corresponding to low, medium or high risk was assigned as follows based on the risk of developing T1D: Age: >40 (0); 30-40 (1); 0-30 (2). HLA: No risk alleles (0); DR4 or DR3 only (1); DR4 DQ8 or DR3 DQ2 or DQ8 (2). Autoantibodies: 0 (0); 1 (1), 2 (2). The Risk Index was then calculated as the sum of the values obtained in each category for each donor (range 0 (minimum) to 6 (maximum)). There was a strong positive correlation between the risk index and the PI/INS area ratio (right panel) while there was a weak correlation with proinsulin area (central panel) and no correlation with insulin area (left panel) (Supplementary figure 3).

Patients with recent onset type 1 diabetes have more glucagon, less insulin and less proinsulin area but increased proinsulin to insulin area ratio.

To investigate the timing of the increase in proinsulin area and the inversion of the PI/INS area ratio when compared with control donors, pancreas tissue from a set of recently diagnosed patients with type 1 diabetes (0-9 weeks post-diagnosis) was studied (Figure 5). Only the tail region was analyzed, as all but one sample were obtained by tail resection as described in (30) (one section from a donor with type 1 diabetes at onset obtained from nPOD was also included for comparison). Patients with type 1 diabetes were compared to controls, and single and double Ab+ donors separately (Figure 5A). The insulin and proinsulin areas were lower than in the rest of the groups due to a reduction in the islets that contained insulin, whereas there was an increase in glucagon area (Figure 5C, 5D and 5F). Interestingly, the PI/INS area ratio was increased in patients with type 1 diabetes and almost identical to that of at risk, double Ab+ donors (0.77 ± 0.13 controls vs 0.99 ± 0.15 single Ab+ vs 1.06 ± 0.10 double Ab+ vs 1.07 ± 0.18 type 1 diabetes) (Figure 5E left panel).

Systematic analysis of islet size reveals heterogeneity within the pancreas and subtle differences between Ab+ donors and controls.

Small morphological alterations as well as in differences in islet number, size and distribution might occur many years before diagnosis, in individuals at risk of developing disease. First, the number of islets was counted and the total area of the tissue section was measured (see methods for details and Supplementary Figure 1). Total islet number and tissue size were variable across the pancreas but were similar in control and Ab+ donors (data not shown). There were no major differences in mean islet density between non-diabetic (head 2.5 ± 0.5 vs body 1.8 ± 0.2 vs tail 2.8 ± 0.7 islets/mm^2) and Ab+ donors (head 2.6 ± 0.7 vs body 2.1± 0.7 vs tail 3.1 ± 0.9 islets/mm^2) (Figure 6A). Next, the islet size distribution was analyzed. Significant differences were found between non-diabetic controls and double Ab+ donors for the head, body and tail (Figure 6B, Supplementary Figure 4). Lastly, sections from patients with type 1 diabetes were analyzed. Larger islets were found in these sections (Figure 5A and Supplementary Figure 4, tail region only), while the islet density was lower (Figure 5B), as expected. Interestingly, the tail of the pancreas presented a distinct islet distribution compared with the head and body regions for all groups, with a predominance of large islets and fewer small islets (Figure 6C, Supplementary Figure 4), confirming important regional differences within the pancreas.

Changes in the number of alpha and beta cells occur during the pre-diabetic phase and after onset of disease.

The number of insulin and glucagon expressing cells per islet was counted and the ratio between both cell populations was calculated (Supplementary Figure 5A). While no

significant differences were found, double Ab+ donors presented higher beta to alpha cell ratios in head, body and tail regions (Head median = 3.8 control vs 5.3 single Ab+ vs 6.4 double Ab+ / body median = 4.0 control vs 3.8 single Ab+ vs 7.1 double Ab+ / tail median = 3.6 control vs 3.8 single Ab+ vs 4.9 double Ab+). Amongst the Ab+ donors, very heterogeneous cell distribution patterns were found, with some individuals having a higher abundance of alpha cells per islet (Supplementary Figure 5B central panel) and others with a clear predominance of beta cells (Supplementary Figure 5B right panel) when compared with control sections (Supplementary Figure 5B left panel).

Patients with type 1 diabetes had a significantly lower beta to alpha cell ratio (median = 1.1 type 1 diabetes, tail region only) (Figure 5E right panel). Lastly, the percentage of islets containing only beta cells was calculated, which again, was similar for the control (24.9% ± 9.0), single (28.8% ± 9.9) and double Ab+ group (31.3% ± 16.8), and lower for the type 1 diabetes group (3.5% ± 4.9) (Figure 5G left panel). Islets with only alpha cells were not common (control 3.5% ± 3.2 vs single Ab+ 2.8% ± 0.8 vs double Ab+ 5.2% ±7.7). Only one double Ab+ donor (# 6267, 18.9%) and the donors with type 1 diabetes (52.2% ± 22.4) presented evident increases in the percentage of islets containing only alpha cells when compared with the rest of the donor groups (Figure 5G, right panel).

DISCUSSION

The recent access to human pancreata for research purposes and the subsequent histological studies have filled important gaps in our understanding of pancreatic pathology (10; 31-33). However, many fundamental questions remain to be answered. In this study, we aimed to fully characterize beta and alpha cells, investigating insulin, proinsulin and

glucagon content and distribution across head, body and tail regions of the human pancreas in healthy individuals and single as well as multiple Ab+ donors. In addition, we had access to a very unique subset of pancreatic tissues from living patients with recent-onset type 1 diabetes who participated in the DiViD study in which a small piece of the tail of the pancreas was surgically removed immediately in the months following diagnosis (30). Our study is the first to show an increase in pancreatic proinsulin area in prediabetic individuals and confirms the value of the PI/INS area ratio as an indicator of early beta cell dysfunction. In addition, we confirm previous findings that beta cell mass is not reduced in Ab+ individuals. We therefore add critical refinement to the original model of beta cell loss described by Eisenbarth three decades ago (4). We did not find any significant differences in the overall insulin positive area between healthy controls and Ab+ donors to support a reduction in insulin content long before the onset of disease. Moreover, beta cell mass was essentially identical in both groups, demonstrating that beta cells are preserved in Ab+ individuals until shortly before diagnosis and in agreement with previous publications that reported no differences in beta cell mass between non-diabetic and Ab+ donors (34-36).

Increases in proinsulin area were found in some of the single Ab+ pancreata, which could explain why the first phase insulin response is already abnormal in some of these individuals (4). Proinsulin primarily accumulates in the Golgi apparatus in resting beta cells and is further processed to insulin and C-peptide in immature secretory granules (37). Our data show~~s~~ significant increases in the proinsulin area in Ab+ individuals in the head, body and tail regions of the pancreas. Using a high-resolution confocal microscope to study a subset of samples, we observed that the increase in the proinsulin area was partially due to a shift in proinsulin subcellular localization, from the Golgi area in controls (juxta-nuclear)

to secretory vesicles in multiple Ab+ individuals (cytosolic). Although an increase in proinsulin area suggests an increase in the amount of proinsulin protein, additional experiments are needed to accurately measure the protein content. Nevertheless, this increase in area could be due to an increase in proinsulin production (to cover insulin demand), or to a defect in the processing and maturation of the existing pool of proinsulin to insulin, which is consequently released to the circulation. This is in agreement with studies which have detected proinsulinemia in prediabetic patients and patients with type 1 diabetes (38). In addition, an increase in proinsulin synthesis could lead to ER stress, protein misfolding and loss of glucose-stimulated insulin secretion (39). Other extrinsic factors, for example recurrent autoimmune attacks or other forms of metabolic stress (40; 41) may affect beta cell function and proinsulin processing early in the prediabetic disease process. In normal beta cells, up to 20% of proinsulin can be misfolded. However, only under pathological conditions and ER dysfunction, and once a certain level of misfolded proinsulin has been accumulated, beta cell toxicity and death can occur (22).

In a case-control study analysis by Sims and colleagues (42) an elevation of the proinsulin to C-peptide (PI/C) ratio preceded disease onset in high-risk subjects, and could be detected at least 12 months prior to diagnosis (42). This is in agreement with the data presented here, in which Ab+ individuals had an increase of the pancreatic PI/INS area ratio. Amongst the single Ab+ group, two donors (case 6170 and case 6184) consistently presented elevated PI/INS area ratio. This suggests that beta cells in these two individuals could have had a functional defect. Conversely, all but one double Ab+ donor (# 6080) presented an increased ratio in at least two of the three regions of the pancreas, supporting the notion of an early functional defect in beta cells during the prediabetic phase and prior

to diagnosis that does not necessarily imply beta cell loss. Donor 6080 was positive for Glutamic Acid Decarboxylase (GAD) and insulin autoantibodies but was 69 years old and therefore, unlikely to have developed the disease. In conclusion, our results, *in situ*, correlate well with those found in serum and confirm the potential of monitoring PI/C or PI/INS ratios as indicators of beta cell dysfunction.

The samples obtained from living individuals with recent-onset type 1 diabetes through the DiViD study (30) showed an expected significant decrease in the insulin and proinsulin area due to a reduced number of insulin-containing islets, however 4 out of 6 patients had elevated PI/INS area ratios suggesting that insulin therapy at onset might not fully alleviate the dysfunctional beta cells. Our findings indicate that potential therapies should target beta cells early before onset, when they still have the ability to be functionally rescued and when the immune system has not been fully activated.

We further characterized islet distribution and composition in order to study if small differences in islet pathology could be observed early in the prediabetic phase. The tail of the pancreas contained larger islets and higher islet density in all donor groups, which could point to important developmental and architectural differences in vascularization and innervation of the islets in this region (43; 44). Interestingly, subtle differences were found in double Ab+, at risk, individuals, in which larger islets were found in the body and tail region of the pancreas compared with controls. Moreover, this tendency was accentuated in recently diagnosed individuals with type 1 diabetes, where even larger islets could be found in the tail region, many of them containing only alpha cells. This is in agreement with previous studies in diabetic NOD mice in which small islets were preferentially lost and a

subsequent expansion of large islets was seen (45). An increase in the size of the islet and number of beta cells in multiple Ab+ donors could be a compensatory mechanism due to the chronic increase in insulin demand.

Our observations in the pancreas of individuals at risk of developing type 1 diabetes point to important and very early (at the first sign of autoimmunity) pathological changes in beta cells without an evident loss of beta cell mass. This confirms the potential benefit of estimating the PI/C or PI/INS ratios in Ab+ individuals in order to identify those patients at high risk at a stage where beta cells might still respond to preventive therapies and in order to enroll patients in clinical trials at a point in the disease when they would benefit the most. Whether a consequence of an increase in insulin demand, a primary cellular defect or a change in the orchestrated interplay between the immune system and the islet, the higher accumulation of proinsulin in beta cells without a reduction in insulin content might ultimately lead to beta cell exhaustion and death, with the subsequent release of beta cell antigens which initiate the autoimmune process. Whether type 1 diabetes is a primary autoimmune disease or autoimmunity is secondary to metabolic or functional defects that render beta cells susceptible to autoimmune destruction remains unknown. Future studies on proinsulin and insulin dynamics as well as a better characterization of beta cells themselves will provide the necessary answers to fully understand the pathological changes that precede the clinical onset of type 1 diabetes.

ACKNOWLEDGMENTS: This research was performed with the support of nPOD, a collaborative type 1 diabetes research project sponsored by the Juvenile Diabetes Research Foundation International (JDRF). Organ Procurement Organizations, partnering with nPOD to provide research resources, are listed at www.jdrfnpod.org/our-partners.php. The proinsulin antibody clone GS-9A8, developed by Madsen, O.D. was obtained from the Developmental Studies Hybridoma Bank, created by the NICHD of the NIH and maintained at The University of Iowa, Department of Biology, Iowa City, IA 52242. We would like to thank Zbigniew Mikulsky and Bill Kiosses of La Jolla Institute for Allergy and Immunology for their help with image acquisition and analysis, and Priscilla Colby of La Jolla Institute for Allergy and Immunology for administrative assistance

FUNDING: This study was supported by National Institutes of Health/National Institute of Allergy and Infectious Diseases Grant R01 AI092453-03.

DUALITY OF INTEREST: M.G.v.H. is an employee of Novo Nordisk. No other potential conflicts of interest relevant to this article were reported.

AUTHOR CONTRIBUTIONS: T.R-C. performed and designed experiments, analyzed and interpreted data, and wrote the manuscript. J.Z-G. designed the custom macros developed for computer assisted software analysis, analyzed and interpreted data using bioinformatics tools and helped with statistical analysis. N.A. performed experiments. E.C and Y.L helped with analysis. L.K, and K.D-J. collected patient material and revised the manuscript; K.D-J. is Principal Investigator of the DiViD study. M.v.H. designed experiments, interpreted data, and wrote the manuscript. M.v.H. is the guarantor of this work and, as such, had full access to all the data in the study and takes responsibility for the integrity of the data and the accuracy of the data analysis.

PRIOR PRESENTATION: Preliminary results from this study were presented at the Immunology of Diabetes Society 14th International Congress, Munich, Germany, 12-16 April 2015; the nPOD 8th Annual Scientific Meeting, Miami, FL, 22-25 February 2016; the 52nd Eruopean Association for the Study of Diabetes (EASD) Annual Meeting, Munich, Germany, 12-16 September 2016 and the 19th Inflammation Research Association (IRA)

International Meeting, San Diego, USA, 20-21 September 2016.

Tables

Table 1: Donor demographic information including age, percentage of males and females, ethnicity, BMI, disease duration and C-peptide levels.

	Control	Ab+	T1D	Total
n	9	13	7	29
Age (years) mean (±SD)	33.6 (±12.5)	36.1 (±13.5)	28.2 (±4.9)	32.6 (±4.1)
Female (%)	4 (44.5)	8 (61.5)	3 (42.8)	15 (51.7)
Male (%)	5 (55.5)	5 (38.5)	4 (57.2)	14 (48.3)
Ethnicity (%)				
African American	0 (0)	2 (15.4)	0 (0)	2 (6.9)
Caucasian	7 (77.7)	8 (61.5)	7 (100)	22 (75.9)
Hispanic	2 (22.3)	3 (23.1)	0 (0)	5 (17.2)
BMI mean (±SD)	28.2 (±6)	26.2 (±5)	25 (±3.2)	26.5 (±1.6)
Disease duration in weeks (±SD)			4.4 (±2.7)	
C-peptide (ng/ml) mean (±SD)	6.7 (±7.2)	6.1 (±6.2)	--------	

Figure legends:

Figure 1: *Proinsulin area but not insulin area is significantly increased in the pancreas of autoantibody positive donors compared with non-diabetic controls.* Insulin (left panel), proinsulin (middle panel) and glucagon (right panel) areas expressed as percentage of positive area were measured in whole tissue sections from the head **(A)**, body **(B)** and tail **(C)** region of the pancreas obtained from non-diabetic controls (n=9, black circles); single (n=8, black squares) and double (n=5, open squares) non-diabetic autoantibody positive cadaveric organ donors. * $p \leq 0.05$; ** $p \leq 0.01$.

Figure 2: *Proinsulin accumulates in the cytoplasmic compartment in beta cells from autoantibody positive donors.* Pancreatic sections from control (upper rows), single (middle rows) and double (lower rows) non-diabetic Ab+ cadaveric organ donors were stained for insulin (green), proinsulin (red), glucagon (white) and DAPI (blue) following a standard immunofluorescence staining protocol. The merged image can be seen on the right panel. Images were taken using a ZEISS LSM 880 confocal with Airyscan and a 63x objective. Scale bar 10µm.

Figure 3: *Beta cell mass is not reduced in single or double autoantibody positive donors*
A) Beta cell mass calculated as total pancreas weight multiplied by insulin area in non-diabetic controls, single and double non-diabetic autoantibody positive donors. **B)** Beta cell mass calculated as total pancreas weight multiplied by proinsulin area in non-diabetic controls, single and double non-diabetic autoantibody positive donors. **C)** Alpha cell mass calculated as total pancreas weight multiplied by glucagon area in non-diabetic controls, single and double non-diabetic autoantibody positive donors. All panels: Non-diabetic controls (n=9, black circles), single (n=8, black squares) and double (n=5, open squares) non-diabetic Ab+ cadaveric organ donors. * $p \leq 0.05$.

Figure 4: *The proinsulin to insulin area ratio is increased in autoantibody positive donors and constitutes a potential indicator of beta cell dysfunction.* **A)** The ratio between proinsulin and insulin area (PI/INS area ratio) was calculated for head (left panel), body (middle panel) and tail (right panel) regions of the pancreas from non-diabetic controls, single and double non-diabetic Ab+ donors. **B)** Proinsulin area versus insulin area XY plot: a theoretical reference value of 1:1

(proinsulin : insulin) was chosen and graphically represented as a line capable of separating control from "at risk" donors. The area under this line represents a ratio smaller than 1 and viceversa. The distance from the donor's area values to the line was used as a score to estimate the risk of developing disease and used to classify and distinguish control from Ab+ (single and double combined). **C)** Receiver Operating Characteristic (ROC) for the head (left panel), body (middle panel) and tail (right panel) regions of the pancreas; the Area Under the Curve (AUC) was calculated for the classifier described in B). The p-values show the significance of the logistic regression model including the predictor when compared to a model with just the intercept. Non-diabetic controls (n=9, black circles), single (n=8, black squares) and double (n=5, open squares) non-diabetic Ab+ cadaveric organ donors. ** $p \leq 0.01$; *** $p \leq 0.001$.

Figure 5: *Higher glucagon, lower insulin and proinsulin areas but increased proinsulin to insulin area ratio in recent onset type 1 diabetic patients.* **A)** Boxplots represent islet size distribution for non-diabetic controls (HC, n=5109), single (SingleAb, n=4692), double Ab+ (doubleAb, n=2859) and T1D (T1D, n=1748) donors in tail region of the pancreas. **B)** Islet density was calculated as the total number of islets per section divided by the total area of the tissue for the tail region of the pancreas. **C)** Representative image from whole tissue section of donor #6362, with type 1 diabetes, at onset. Insulin is shown in green, glucagon in red and DAPI in blue. Note the presence of insulin-deficient and insulin-containing islets scattered across the pancreas parenchyma. **D)** Insulin (left panel), proinsulin (middle panel) and glucagon (right panel) areas expressed as percentage of positive area were measured in whole tissue sections from the tail region of the pancreas. **E)** The proinsulin to insulin area ratio (PI/INS area ratio; left panel) and the beta to alpha cell ratio (right panel) were calculated for the pancreas tail region. **F)** Representative image of an islet from a recent-onset donor (DiViD study). Insulin is shown in green, proinsulin in red and glucagon in blue. **G)** The percentage of islets containing only beta cells (left panel) and only alpha cells (right panel) is shown. All panels: Non-diabetic controls (n=9, black circles), single (n=8, green squares), double (n=5, red squares) non-diabetic Ab+ and type 1 diabetes donors (n=7, blue triangles). * $p \leq 0.05$; ** $p \leq 0.01$; *** $p \leq 0.001$; **** $p \leq 0.0001$. Scale bar 500 μm in C) and 50 μm in F).

Figure 6: *Systematic analysis of islet distribution reveals heterogeneity within the pancreas and subtle differences between Ab+ donors and controls.* **A)** Islet density was calculated as the

total number of islets per section divided by the total area of the tissue for head, body and tail regions of the pancreas. Black circles represent control donors (n=9) while single Ab+ are shown in black squares (n=8) and double Ab+ in open squares (n=5). **B)** Boxplots represent islet size distribution for healthy controls, single and double Ab+ donors in head (left panel), body (middle panel) and tail (right panel) region of the pancreas. **C)** Boxplots represent islet size distribution for head, body and tail regions in healthy controls (left panel), single (middle panel) and double (right panel) Ab+. Number of islets: Head (HC n=4390; SingleAb n=4021, DoubleAb n=2067), body (HC n=3446; SingleAb n=4052, DoubleAb n=2043) and tail (HC n=5109; SingleAb n=4692, DoubleAb n=2859). * $p \leq 0.05$; ** $p \leq 0.01$; *** $p \leq 0.001$; **** $p \leq 0.0001$.

Supplementary Table 1: *Extended donor information*. Table S1 shows extended demographic and histological information, as well as the pancreatic regions analyzed for each donor. Autoab Pos, autoantibody positive donor. T1D, type 1 diabetic donor. Age and duration of disease are expressed in years unless otherwise indicated; BMI, body mass index; C-peptide is expressed in ng/ml; time ICU, time spent in the Intensive Care Unit (in days); ZnT8A, zinc transporter 8 autoantibodies; IA-2A, intracytoplasmic domain of the tyrosine phosphatase IA-2 autoantibodies; mIAA, micro assay for insulin autoantibodies; GADA, glutamic acid decarboxylase 65 autoantibodies. – Indicates not determined or not available.

Supplementary Figure 1: *Image acquisition and analysis.* All sections were scanned with an Axio Scan Z.1 slide scanner (Carl Zeiss microscopy, Thornwood, NY). A) For automated and systematic analysis, custom macros were developed to measure tissue area (macro #1, B middle panels); islet size and count (macro #2, B lower panels); calculate insulin, proinsulin and glucagon areas (macro #3, B upper panels). To classify and count alpha and beta cells, the image of the whole tissue section was exported into 20x20 smaller images in order to improve resolution, and then processed by a different custom macro (macro #4, C). Scale bar 500 μm in B and 50 μm in C.

Supplementary Figure 2: *Increase in proinsulin area and change in its subcellular localization without evident insulin depletion in autoantibody positive individuals.* High-resolution images and two-dimensional graphs of the intensities of pixels along the corresponding images from

control, single and double Ab+ donors. A column average plot is displayed representing the horizontal distance through the image (in μm) and the average pixel intensity for: A) proinsulin (red profile) and B) insulin (green profile). Scale bar 10 μm.

Supplementary figure 3: *Risk index*. Table: To calculate the Risk Index, a score of 0, 1 or 2 corresponding to low, medium or high risk was assigned as follows based on the risk of developing T1D: Age: >40 (0); 30-40 (1); 0-30 (2). HLA: No risk alleles (0); DR4 or DR3 only (1); DR4 DQ8 or DR3 DQ2 or DQ8 (2). Autoantibodies: 0 (0); 1 (1), 2 (2). The Risk Index was then calculated as the sum of the values obtained in each category for each donor (range 0 (minimum) to 6 (maximum)). Correlation analyses between the risk index and insulin area, proinsulin area and the PI/INS area ratio are shown for the head, body and tail regions (r and p-value area provided in the graph). Non-diabetic controls (n=9, black circles), single (n=8, green circles) and double (n=5, red circles) Ab+ cadaveric organ donors.

Supplementary Figure 4: *Increase in the size of the islets with autoantibody seroconversion and after onset of disease.* A) The median (table and bar graph) and interquantile range (IQR) of islet size distribution (μm^2) are shown for pancreas head, body and tail regions of control, single Ab+, double Ab+ and type 1 diabetes donors. Note the increase in islet size in double Ab+ and type 1 diabetes compared to controls.

Supplementary Figure 5: *Changes in the number of alpha and beta cells and their distribution in the islet can be observed during the pre-diabetic phase.* **A)** The number of alpha and beta cells per islet was counted and the ratio beta to alpha cell calculated for head (left panel), body (center panel) and tail (right panel) regions of the pancreas. Non-diabetic controls (n=9, black circles), single (n=8, green squares) and double (n=5, red squares) non-diabetic Ab+. **B)** Representative images from insulin (green), proinsulin (orange), glucagon (red) and DAPI (blue) staining on # 6102 control (left panel), # 6267 double Ab+ (center panel) and # 6158 double Ab+ (right panel). Note the different patterns of beta and alpha cell content as well as insulin, proinsulin and glucagon. A) normal pattern, B) predominantly alpha cells and C) predominantly beta cells. Scale bar 100 μm.

REFERENCES

1. Pugliese A: The multiple origins of Type 1 diabetes. Diabetic medicine : a journal of the British Diabetic Association 2013;30:135-146
2. van Belle TL, Coppieters KT, von Herrath MG: Type 1 diabetes: etiology, immunology, and therapeutic strategies. Physiological reviews 2011;91:79-118
3. Srikanta S, Ganda OP, Gleason RE, Jackson RA, Soeldner JS, Eisenbarth GS: Pre-type I diabetes. Linear loss of beta cell response to intravenous glucose. Diabetes 1984;33:717-720
4. Eisenbarth GS: Type I diabetes mellitus. A chronic autoimmune disease. The New England journal of medicine 1986;314:1360-1368
5. Sosenko JM, Skyler JS, Herold KC, Palmer JP, Type 1 Diabetes T, Diabetes Prevention Trial-Type 1 Study G: The metabolic progression to type 1 diabetes as indicated by serial oral glucose tolerance testing in the Diabetes Prevention Trial-type 1. Diabetes 2012;61:1331-1337
6. Helminen O, Aspholm S, Pokka T, Hautakangas MR, Haatanen N, Lempainen J, Ilonen J, Simell O, Knip M, Veijola R: HbA1c Predicts Time to Diagnosis of Type 1 Diabetes in Children at Risk. Diabetes 2015;64:1719-1727
7. Krogvold L, Skog O, Sundstrom G, Edwin B, Buanes T, Hanssen KF, Ludvigsson J, Grabherr M, Korsgren O, Dahl-Jorgensen K: Function of Isolated Pancreatic Islets From Patients at Onset of Type 1 Diabetes: Insulin Secretion Can Be Restored After Some Days in a Nondiabetogenic Environment In Vitro: Results From the DiViD Study. Diabetes 2015;64:2506-2512
8. Marre ML, James EA, Piganelli JD: beta cell ER stress and the implications for immunogenicity in type 1 diabetes. Frontiers in cell and developmental biology 2015;3:67
9. Eizirik DL, Cnop M: ER stress in pancreatic beta cells: the thin red line between adaptation and failure. Science signaling 2010;3:pe7
10. Campbell-Thompson M, Fu A, Kaddis JS, Wasserfall C, Schatz DA, Pugliese A, Atkinson MA: Insulitis and beta-Cell Mass in the Natural History of Type 1 Diabetes. Diabetes 2016;65:719-731
11. Ziegler AG, Rewers M, Simell O, Simell T, Lempainen J, Steck A, Winkler C, Ilonen J, Veijola R, Knip M, Bonifacio E, Eisenbarth GS: Seroconversion to multiple islet autoantibodies and risk of progression to diabetes in children. Jama 2013;309:2473-2479
12. Bonifacio E: Predicting type 1 diabetes using biomarkers. Diabetes care 2015;38:989-996
13. Narendran P, Mannering SI, Harrison LC: Proinsulin-a pathogenic autoantigen in type 1 diabetes. Autoimmunity reviews 2003;2:204-210
14. Thayer TC, Pearson JA, De Leenheer E, Hanna SJ, Boldison J, Davies J, Tsui A, Ahmed S, Easton P, Siew LK, Wen L, Wong FS: Peripheral Proinsulin Expression Controls Low-Avidity Proinsulin-Reactive CD8 T Cells in Type 1 Diabetes. Diabetes 2016;65:3429-3439
15. Pearson JA, Thayer TC, McLaren JE, Ladell K, De Leenheer E, Phillips A, Davies J, Kakabadse D, Miners K, Morgan P, Wen L, Price DA, Wong FS: Proinsulin Expression Shapes the TCR Repertoire but Fails to Control the Development of Low-Avidity Insulin-Reactive CD8+ T Cells. Diabetes 2016;65:1679-1689
16. Toma A, Laika T, Haddouk S, Luce S, Briand JP, Camoin L, Connan F, Lambert M, Caillat-Zucman S, Carel JC, Muller S, Choppin J, Lemonnier F, Boitard C: Recognition of human proinsulin leader sequence by class I-restricted T-cells in HLA-A*0201 transgenic mice and in human type 1 diabetes. Diabetes 2009;58:394-402
17. Toma A, Haddouk S, Briand JP, Camoin L, Gahery H, Connan F, Dubois-Laforgue D, Caillat-Zucman S, Guillet JG, Carel JC, Muller S, Choppin J, Boitard C: Recognition of a

subregion of human proinsulin by class I-restricted T cells in type 1 diabetic patients. Proceedings of the National Academy of Sciences of the United States of America 2005;102:10581-10586
18. Mallone R, Martinuzzi E, Blancou P, Novelli G, Afonso G, Dolz M, Bruno G, Chaillous L, Chatenoud L, Bach JM, van Endert P: CD8+ T-cell responses identify beta-cell autoimmunity in human type 1 diabetes. Diabetes 2007;56:613-621
19. Michels AW, Landry LG, McDaniel KA, Yu L, Campbell-Thompson M, Kwok WW, Jones KL, Gottlieb PA, Kappler JW, Tang Q, Roep BO, Atkinson MA, Mathews CE, Nakayama M: Islet-derived CD4 T-cells targeting proinsulin in human autoimmune diabetes. Diabetes 2016;
20. Babon JA, DeNicola ME, Blodgett DM, Crevecoeur I, Buttrick TS, Maehr R, Bottino R, Naji A, Kaddis J, Elyaman W, James EA, Haliyur R, Brissova M, Overbergh L, Mathieu C, Delong T, Haskins K, Pugliese A, Campbell-Thompson M, Mathews C, Atkinson MA, Powers AC, Harlan DM, Kent SC: Analysis of self-antigen specificity of islet-infiltrating T cells from human donors with type 1 diabetes. Nature medicine 2016;22:1482-1487
21. Liu M, Wright J, Guo H, Xiong Y, Arvan P: Proinsulin entry and transit through the endoplasmic reticulum in pancreatic beta cells. Vitamins and hormones 2014;95:35-62
22. Sun J, Cui J, He Q, Chen Z, Arvan P, Liu M: Proinsulin misfolding and endoplasmic reticulum stress during the development and progression of diabetes. Molecular aspects of medicine 2015;42:105-118
23. de Beeck AO, Eizirik DL: Viral infections in type 1 diabetes mellitus--why the beta cells? Nature reviews Endocrinology 2016;12:263-273
24. Krogvold L, Edwin B, Buanes T, Frisk G, Skog O, Anagandula M, Korsgren O, Undlien D, Eike MC, Richardson SJ, Leete P, Morgan NG, Oikarinen S, Oikarinen M, Laiho JE, Hyoty H, Ludvigsson J, Hanssen KF, Dahl-Jorgensen K: Detection of a low-grade enteroviral infection in the islets of langerhans of living patients newly diagnosed with type 1 diabetes. Diabetes 2015;64:1682-1687
25. Cianciaruso C, Phelps EA, Pasquier M, Hamelin R, Demurtas D, Ahmed MA, Piemonti L, Hirosue S, Swartz MA, De Palma M, Hubbell JA, Baekkeskov S: Primary Human and Rat Beta Cells Release the Intracellular Autoantigens GAD65, IA-2 and Proinsulin in Exosomes Together with Cytokine-Induced Enhancers of Immunity. Diabetes 2016;
26. Roder ME, Knip M, Hartling SG, Karjalainen J, Akerblom HK, Binder C: Disproportionately elevated proinsulin levels precede the onset of insulin-dependent diabetes mellitus in siblings with low first phase insulin responses. The Childhood Diabetes in Finland Study Group. The Journal of clinical endocrinology and metabolism 1994;79:1570-1575
27. Hartling SG, Knip M, Roder ME, Dinesen B, Akerblom HK, Binder C: Longitudinal study of fasting proinsulin in 148 siblings of patients with insulin-dependent diabetes mellitus. Study Group on Childhood Diabetes in Finland. European journal of endocrinology / European Federation of Endocrine Societies 1997;137:490-494
28. Truyen I, De Pauw P, Jorgensen PN, Van Schravendijk C, Ubani O, Decochez K, Vandemeulebroucke E, Weets I, Mao R, Pipeleers DG, Gorus FK, Belgian Diabetes R: Proinsulin levels and the proinsulin:c-peptide ratio complement autoantibody measurement for predicting type 1 diabetes. Diabetologia 2005;48:2322-2329
29. Watkins RA, Evans-Molina C, Terrell JK, Day KH, Guindon L, Restrepo IA, Mirmira RG, Blum JS, DiMeglio LA: Proinsulin and heat shock protein 90 as biomarkers of beta-cell stress in the early period after onset of type 1 diabetes. Translational research : the journal of laboratory and clinical medicine 2016;168:96-106 e101

30. Krogvold L, Edwin B, Buanes T, Ludvigsson J, Korsgren O, Hyoty H, Frisk G, Hanssen KF, Dahl-Jorgensen K: Pancreatic biopsy by minimal tail resection in live adult patients at the onset of type 1 diabetes: experiences from the DiViD study. Diabetologia 2014;57:841-843
31. Kaddis JS, Pugliese A, Atkinson MA: A run on the biobank: what have we learned about type 1 diabetes from the nPOD tissue repository? Current opinion in endocrinology, diabetes, and obesity 2015;22:290-295
32. Pugliese A, Vendrame F, Reijonen H, Atkinson MA, Campbell-Thompson M, Burke GW: New insight on human type 1 diabetes biology: nPOD and nPOD-transplantation. Current diabetes reports 2014;14:530
33. Campbell-Thompson M: Organ donor specimens: What can they tell us about type 1 diabetes? Pediatric diabetes 2015;16:320-330
34. Wagner R, McNally JM, Bonifacio E, Genovese S, Foulis A, McGill M, Christie MR, Betterle C, Bosi E, Bottazzo GF: Lack of immunohistological changes in the islets of nondiabetic, autoimmune, polyendocrine patients with beta-selective GAD-specific islet cell antibodies. Diabetes 1994;43:851-856
35. In't Veld P, Lievens D, De Grijse J, Ling Z, Van der Auwera B, Pipeleers-Marichal M, Gorus F, Pipeleers D: Screening for insulitis in adult autoantibody-positive organ donors. Diabetes 2007;56:2400-2404
36. Diedisheim M, Mallone R, Boitard C, Larger E: beta-cell Mass in Nondiabetic Autoantibody-Positive Subjects: An Analysis Based on the Network for Pancreatic Organ Donors Database. The Journal of clinical endocrinology and metabolism 2016;101:1390-1397
37. Haataja L, Snapp E, Wright J, Liu M, Hardy AB, Wheeler MB, Markwardt ML, Rizzo M, Arvan P: Proinsulin intermolecular interactions during secretory trafficking in pancreatic beta cells. The Journal of biological chemistry 2013;288:1896-1906
38. Hostens K, Ling Z, Van Schravendijk C, Pipeleers D: Prolonged exposure of human beta-cells to high glucose increases their release of proinsulin during acute stimulation with glucose or arginine. The Journal of clinical endocrinology and metabolism 1999;84:1386-1390
39. Wang S, Kaufman RJ: The impact of the unfolded protein response on human disease. The Journal of cell biology 2012;197:857-867
40. Oresic M, Simell S, Sysi-Aho M, Nanto-Salonen K, Seppanen-Laakso T, Parikka V, Katajamaa M, Hekkala A, Mattila I, Keskinen P, Yetukuri L, Reinikainen A, Lahde J, Suortti T, Hakalax J, Simell T, Hyoty H, Veijola R, Ilonen J, Lahesmaa R, Knip M, Simell O: Dysregulation of lipid and amino acid metabolism precedes islet autoimmunity in children who later progress to type 1 diabetes. The Journal of experimental medicine 2008;205:2975-2984
41. Sysi-Aho M, Ermolov A, Gopalacharyulu PV, Tripathi A, Seppanen-Laakso T, Maukonen J, Mattila I, Ruohonen ST, Vahatalo L, Yetukuri L, Harkonen T, Lindfors E, Nikkila J, Ilonen J, Simell O, Saarela M, Knip M, Kaski S, Savontaus E, Oresic M: Metabolic regulation in progression to autoimmune diabetes. PLoS computational biology 2011;7:e1002257
42. Sims EK, Chaudhry Z, Watkins R, Syed F, Blum J, Ouyang F, Perkins SM, Mirmira RG, Sosenko J, DiMeglio LA, Evans-Molina C: Elevations in the Fasting Serum Proinsulin-to-C-Peptide Ratio Precede the Onset of Type 1 Diabetes. Diabetes care 2016;
43. Amella C, Cappello F, Kahl P, Fritsch H, Lozanoff S, Sergi C: Spatial and temporal dynamics of innervation during the development of fetal human pancreas. Neuroscience 2008;154:1477-1487
44. Lammert E, Cleaver O, Melton D: Induction of pancreatic differentiation by signals from blood vessels. Science 2001;294:564-567

45. Alanentalo T, Hornblad A, Mayans S, Karin Nilsson A, Sharpe J, Larefalk A, Ahlgren U, Holmberg D: Quantification and three-dimensional imaging of the insulitis-induced destruction of beta-cells in murine type 1 diabetes. Diabetes 2010;59:1756-1764

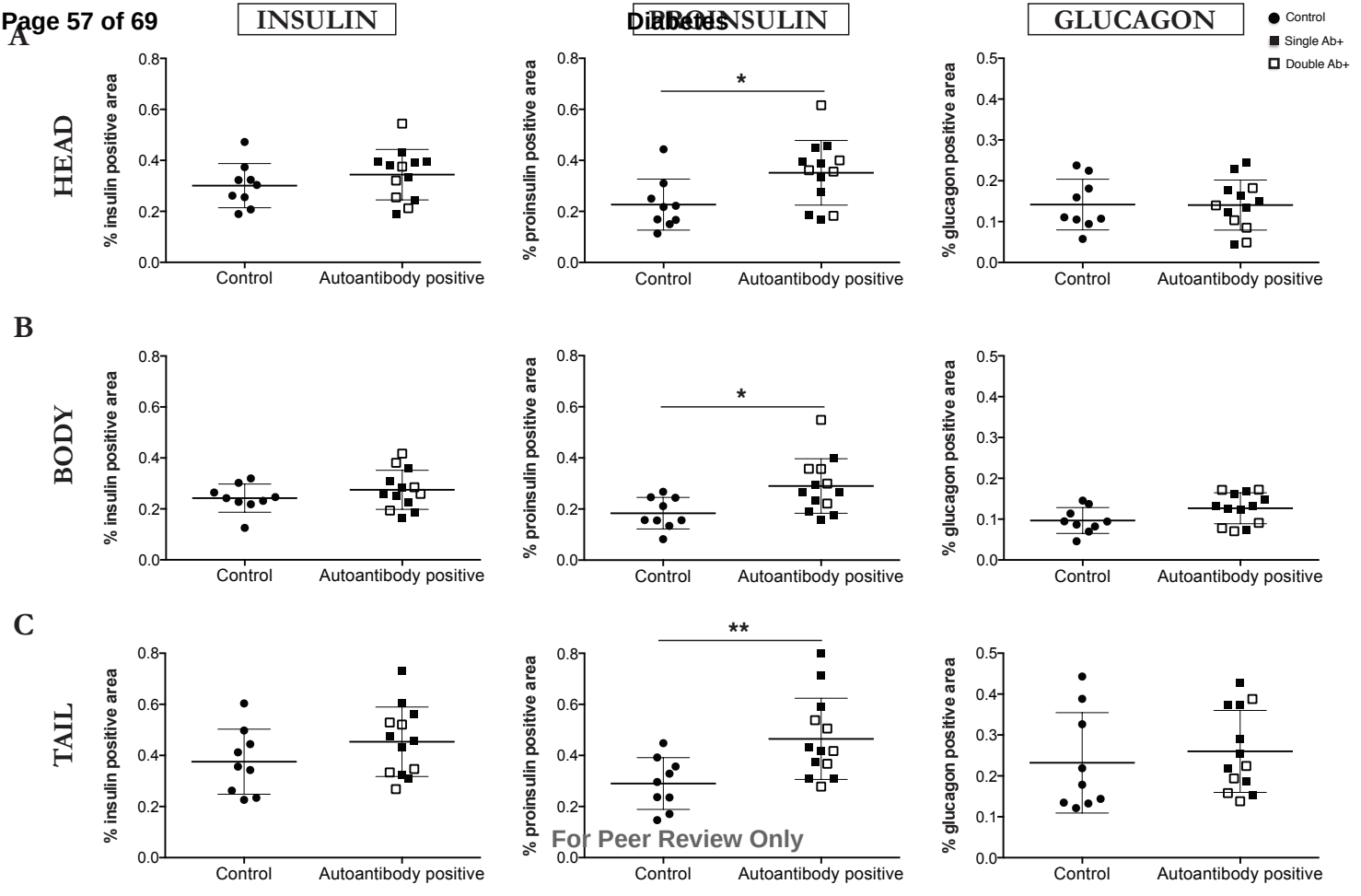
A
B
C
INSULIN
PROINSULIN
GLUCAGON
Control
Single Ab+
Double Ab+
HEAD
BODY
TAIL
% insulin positive area
% proinsulin positive area
% glucagon positive area
Control
Autoantibody positive
*
**
For Peer Review Only

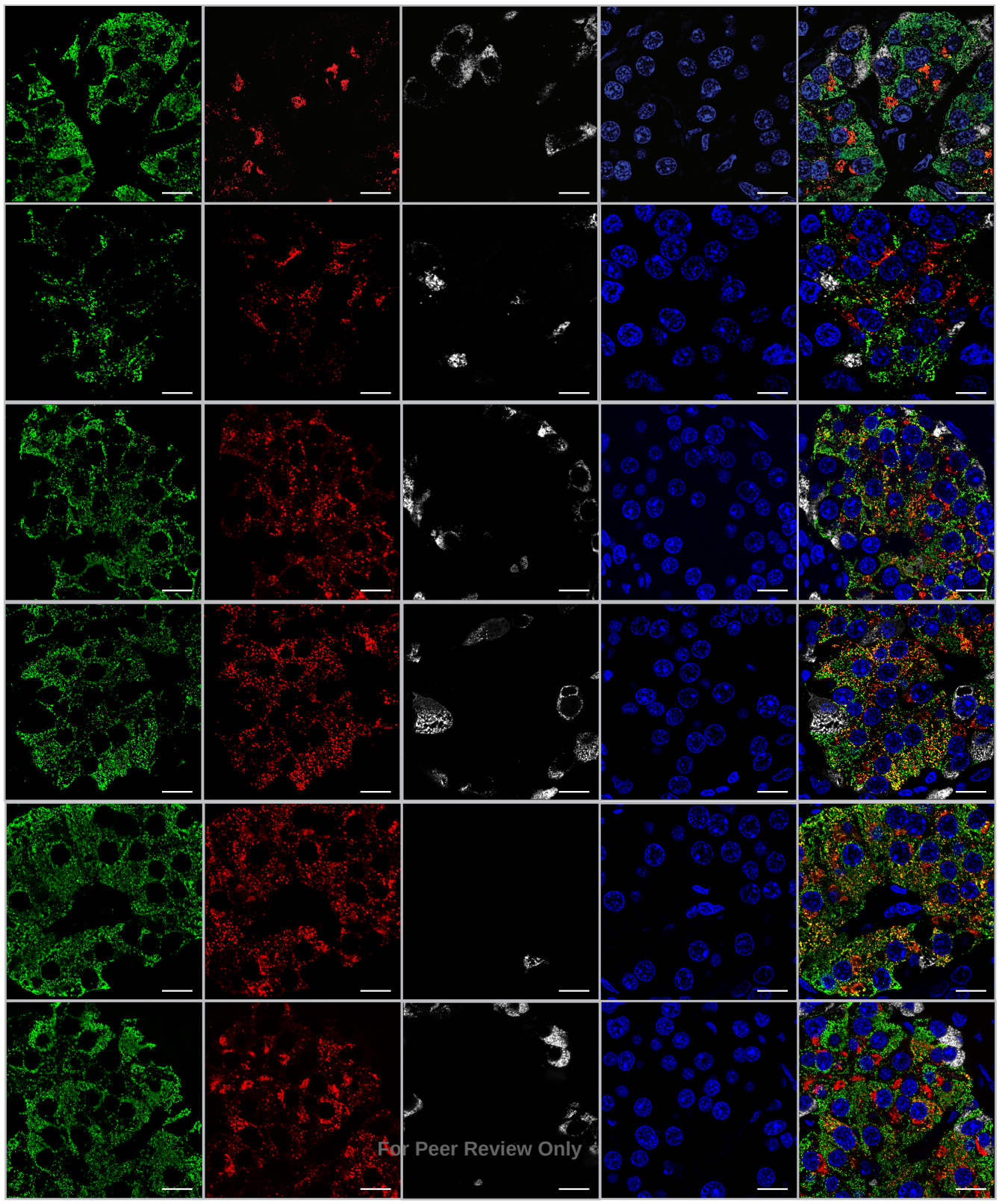

A

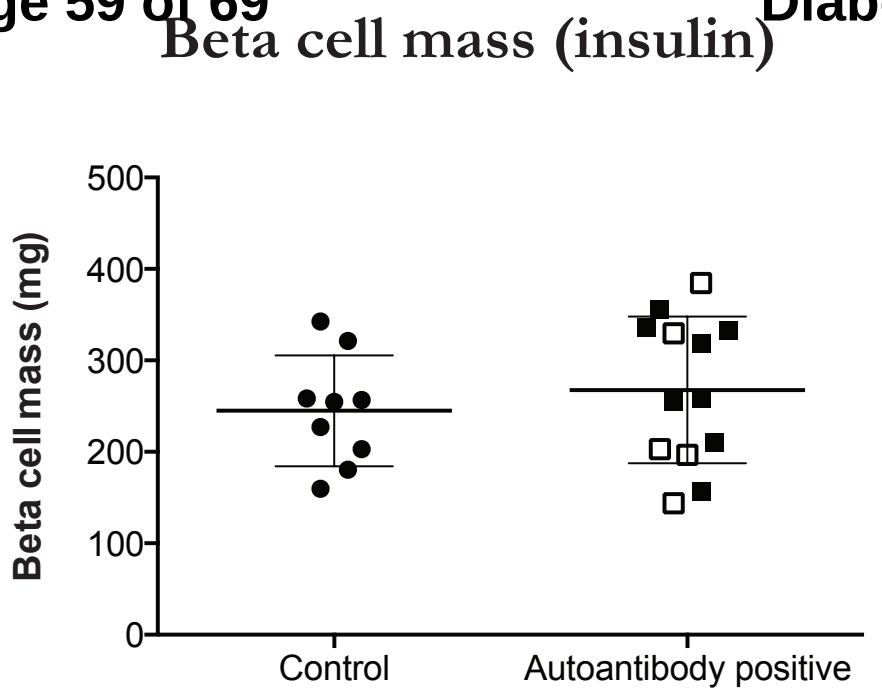

B

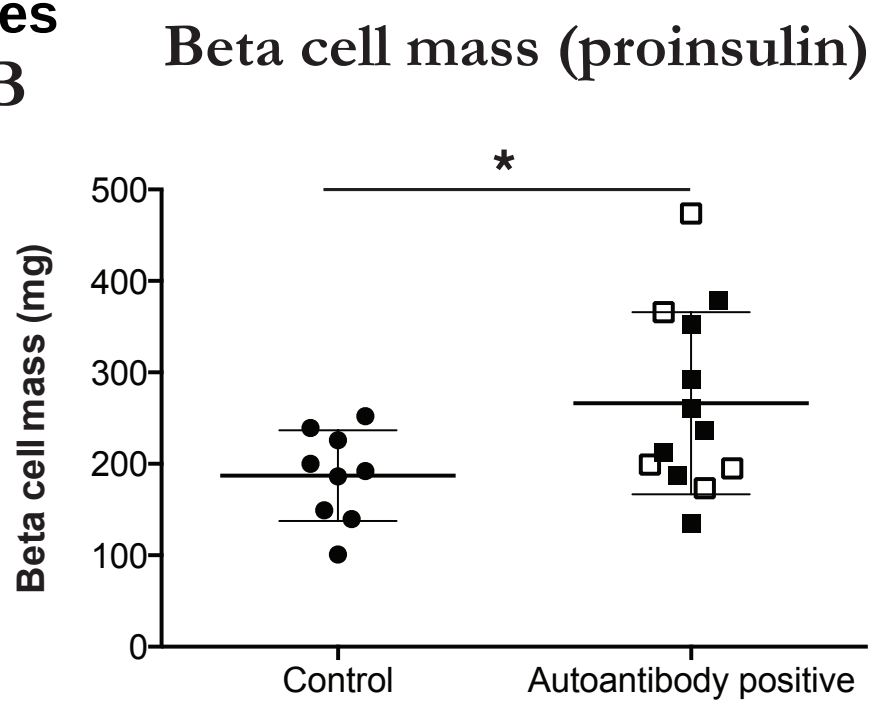

C

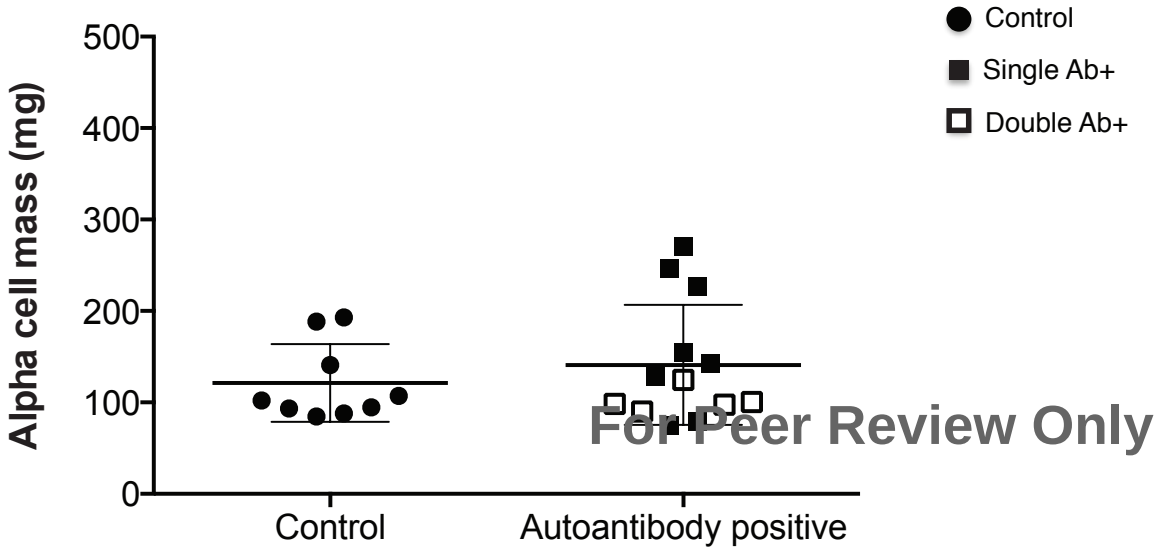

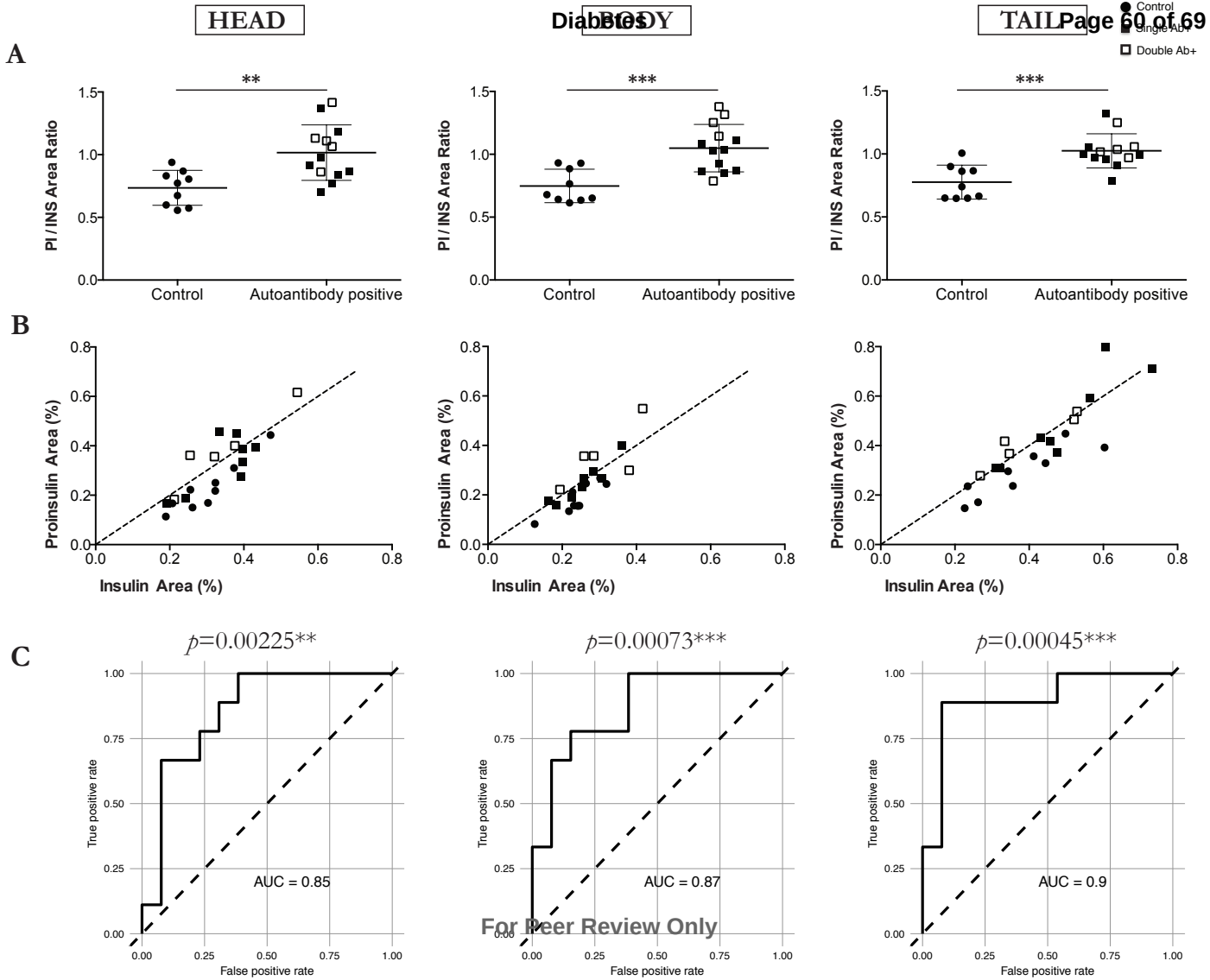

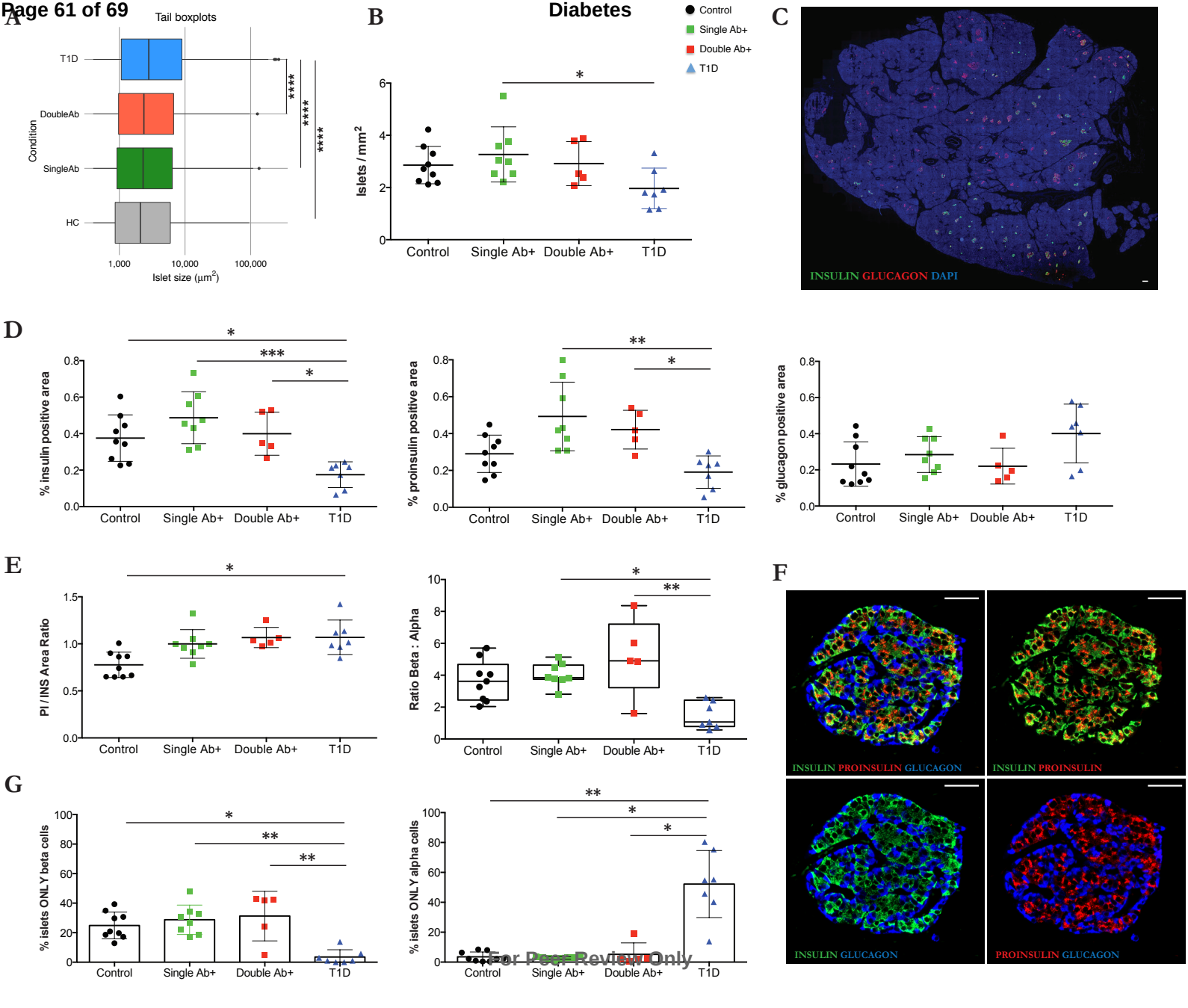

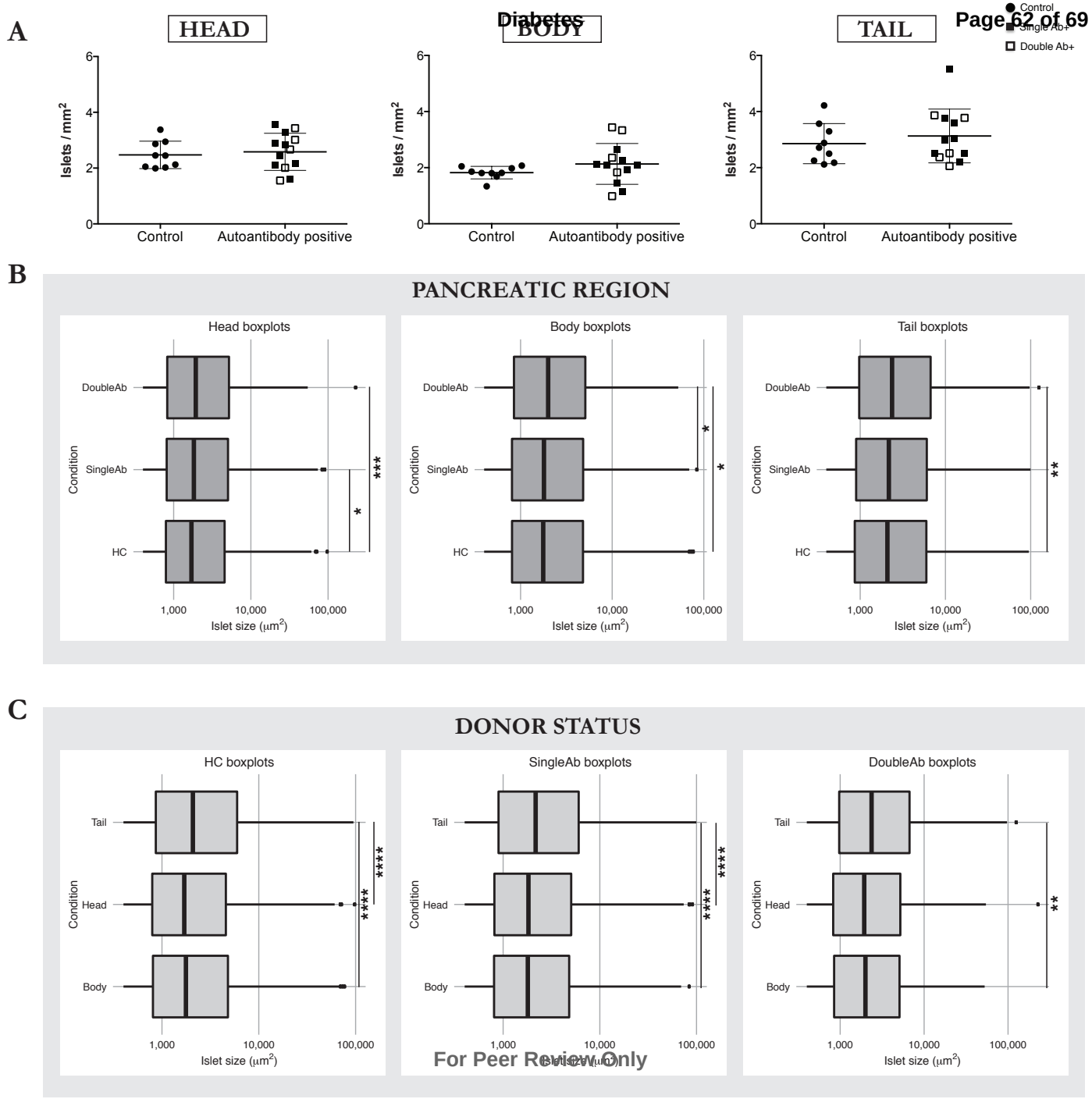

A

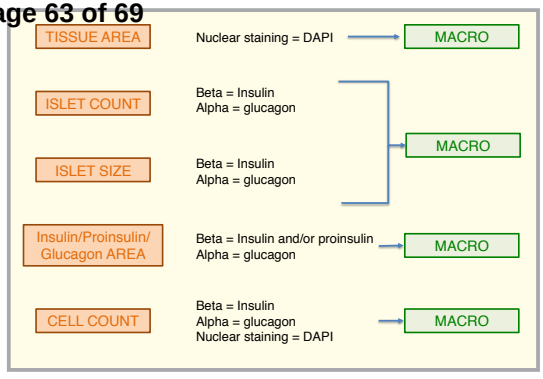

B

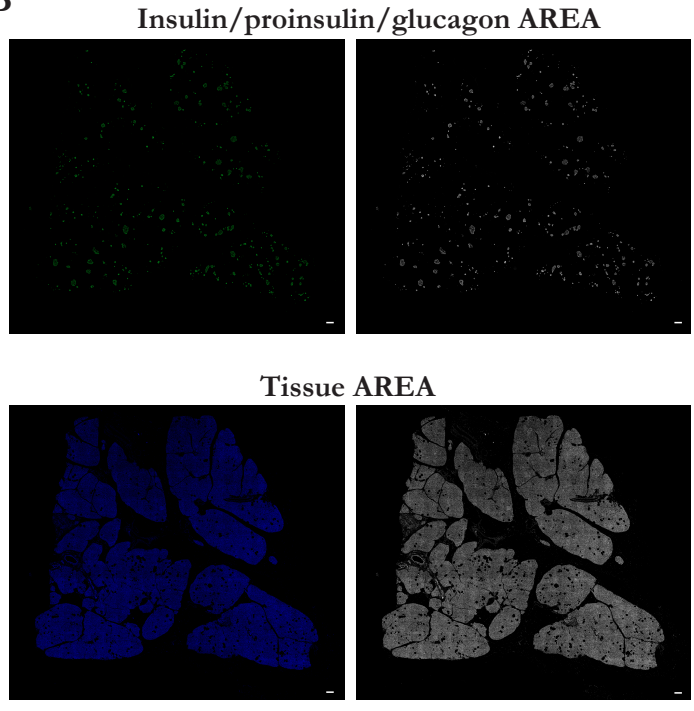

C

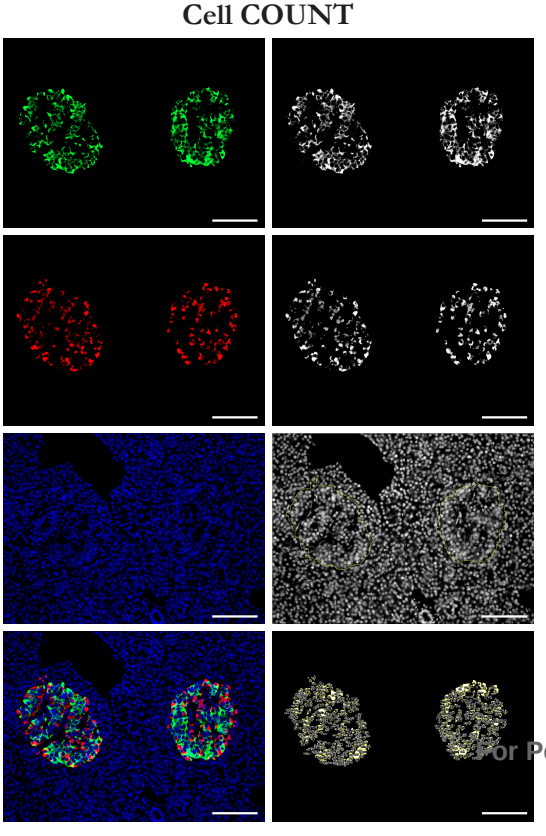

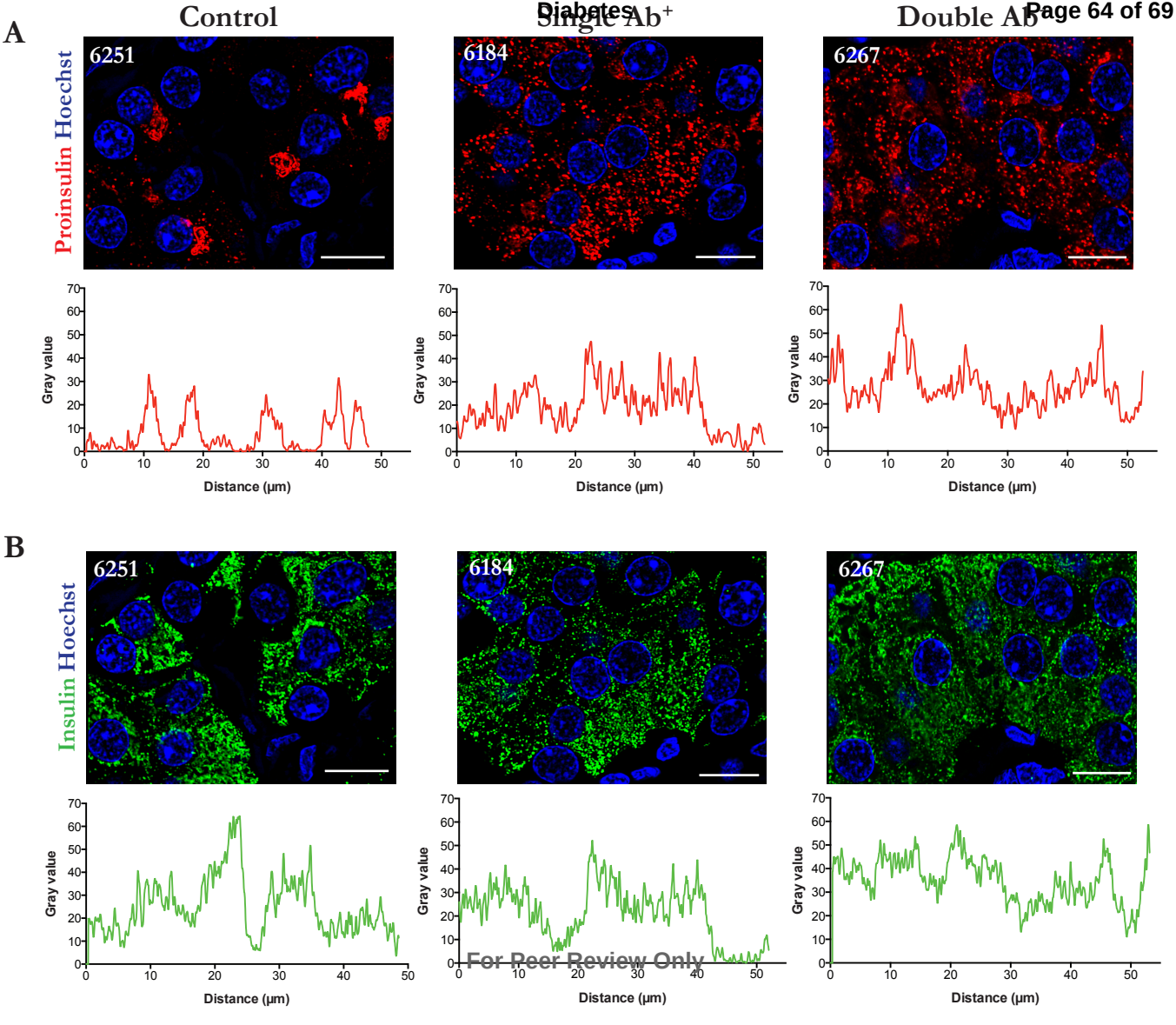

aPOD ID	Donor Type	Age	High resolution HLA	Autoantibodies	RISK index
6044	Autoab Pos	41.4	A*01:01/33:01 B*14:02/37:01 C*06:02/08:02 DRB1*01:02/15:01 DQA1*01:01/01:02 DQB1*05:01/06:02 DPA1*01:03/01:03	1	1
6080	Autoab Pos	69.2	A*02:01/11:01 B*35:01/44:02 C*04:01/05:01 DRB1*01:01/04:01 DQA1*01:01/03:01 DQB1*03:01/05:01 DPA1*01:03/01:03	2	3
6123	Autoab Pos	23.2	A*02:01/24:02 B*35:01/51:01 C*01:02/03:03 DRB1*08:01/11:01 DQA1*04:01/05:01 DQB1*03:01/04:02 DPA1*01:03/01:03 DPB1*04:01/04:01	1	3
6147	Autoab Pos	23.8	A*02:01/02:01 B*08:01/15:01 C*03:04/07:01 DRB1*03:01/04:01 DQA1*03:01/04:01 DQB1*03:01/04:02 DPA1*01:03/02:01 DPB1*01:01/02:01	1	4
6154	Autoab Pos	48.5	A*02:01/03:01 B*07:02/07:02 C*07:02/07:02 DRB1*09:01/15:01 DQA1*01:02/03:01 DQB1*03:03/06:03 DPA1*01:03/01:03 DPB1*02:01/04:01	1	1
6158	Autoab Pos	40.3	A*03:01/24:02 B*15:01/49:01 C*03:04/07:01 DRB1*04:01/13:02 DQA1*01:02/03:01 DQB1*03:01/06:04 DPA1*01:03/01:04 DPB1*04:01:15:01	2	3
6167	Autoab Pos	37	A*01:01, 03:01 DRB1*04:04,15:02 DQA1*01:03,03:01 DQB1*03:02,06:01	2	5
6170	Autoab Pos	34.4	A*29:02,74:01 DRB1*04:01,13:03 DQA1*02:01,03:01 DQB1*02:02,03:01	1	3
6181	Autoab Pos	31.9	A*03:01,11:01 DRB1*01:01,04:01 DQA1*01:01,03:01 DQB1*03:02,05:01	1	4
6184	Autoab Pos	47.6	A*02:06,68:03 DRB1*04:07,04:07 DQA1*03:01,03:01 DQB1*03:02,03:02	1	3
6197	Autoab Pos	22	A*02:02,24:02 DRB1*03:02, 07:01 DQA1*02:01 , 04:01 DQB1*02:02 , 04:02	2	5
6267	Autoab Pos	23	A*01:01, 11:01 DRB1*04:01, 04:04 DQA1*03:01, 03:01 DQB1*03:02, 03:02	2	6
6310	Autoab Pos	28	A*03:01, 30:01 DRB1*07:01, 11:02 DQA1*02:01, 05:01 DQB1*02:02, 03:19	1	3
6029	No diabetes	24	A*03:01/31:02 B*15:15/35:01 C*01:02/04:01 DRB1*04:03/08:02 DQA1*03:01/04:01 DQB1*03:02/04:02 DPA1*01:03/01:03 DPB1*04:02/51:01	0	4
6073	No diabetes	19.2	A*29/01, B*37/44, DR*13/16, DQ*05/06	0	2
6091	No diabetes	27.1	A*01:01/25:01 B*18:01/39:06 C*07:02/12:03 DRB1*08:01/15:01 DQA1*01:02/04:01 DQB1*04:02/06:02 DPA1*01:03/01:03 DPB1*02:01/03:01	0	2
6102	No diabetes	45.1	A*03:01/31:01 B*08:01/44:02 C*05:01/07:01 DRB1*03:01/04:01 DQA1*03:01/05:01 DQB1*02:01/03:01 DPA1*01:03/02:01 DPB1*01:01/02:01	0	2
6104	No diabetes	41	A*29:02/68:01 B*39:06/44:03 C*12:03/16:01 DRB1*07:01/13:01 DQA1*01:01/02:01 DQB1*02:01/05:01 DPA1*01:03/02:02 DPB1*01:01/03:01	0	0
6165	No diabetes	45.8	A*01:01, 02:01 DRB1*13:01, 15:01 DQA1*01:02, 01:03 DQB1*06:02, 06:03	0	0
6168	No diabetes	51	A*02:01, 24:02 DRB1* 01:03, 04:04 DQA1*01:01, 03:01 DQB1*03:02, 05:01	0	2
6251	No diabetes	33	A*02:01, 24:02 DRB1*04:01, 11:01 DQA1*03:01, 05:01 DQB1*03:01, 03:01	0	2
6271	No diabetes	17	A*02:01, 02:06 DRB1*07:01, 15:02 DQA1*01:01, 02:01 DQB1*02:02, 05:01	0	2

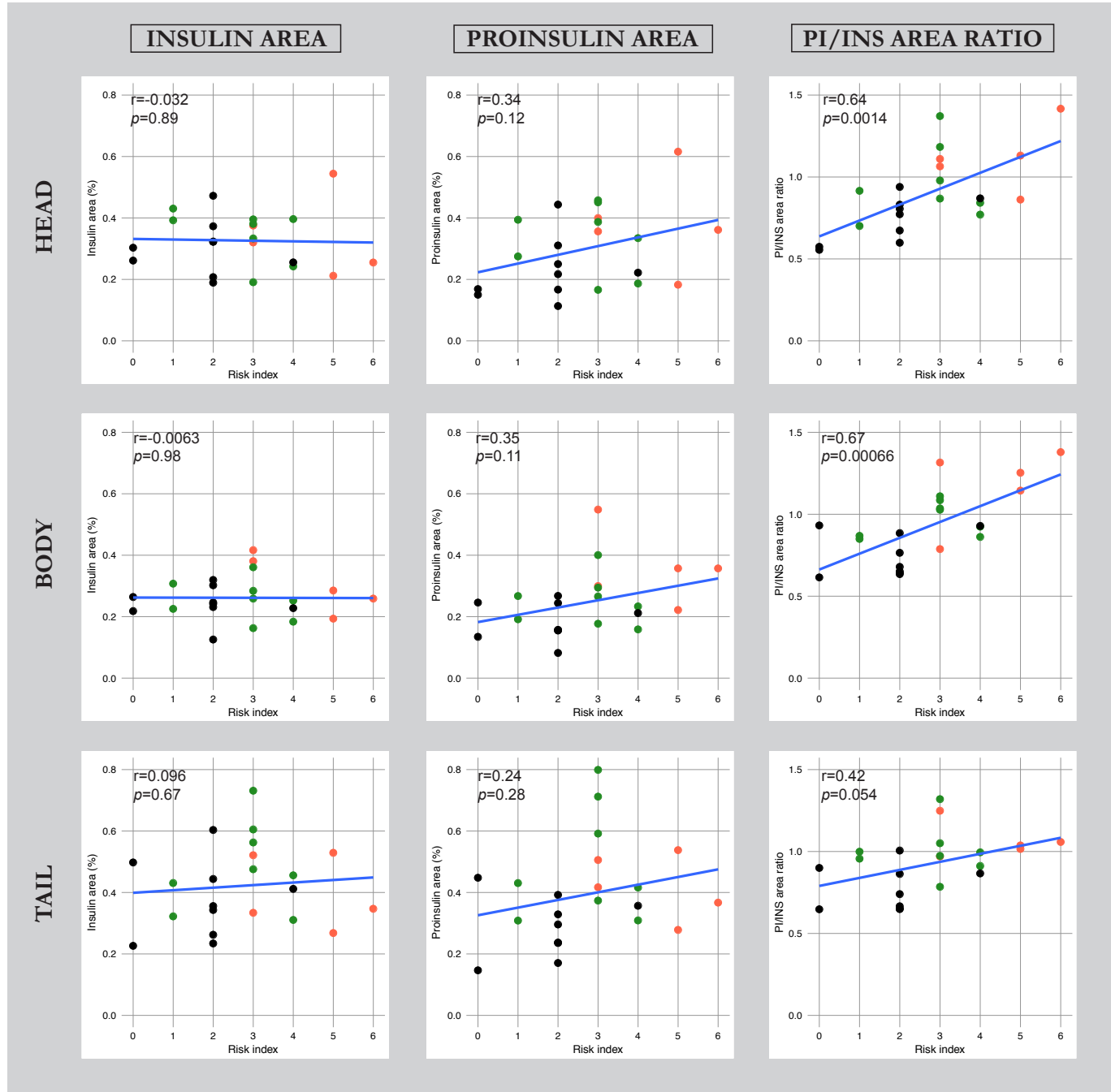

Diabetes

	Control	Single Ab+	Double Ab+	T1D
HEAD	1699.38 (3776.09)	1827.31 (4244.95)	1931.76 (4368.18)	
BODY	1766.87 (3995.14)	1800.32 (4014.63)	1999.83 (4244.36)	
TAIL	2085.46 (5111.26)	2297.93 (5485.75)	2366 (5728.39)	2806.69 (7889.3)

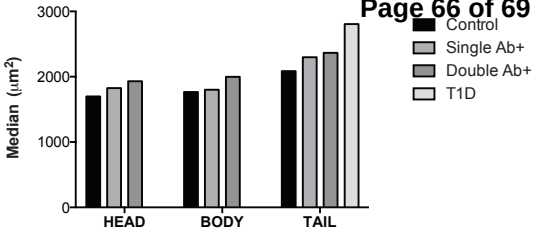

A

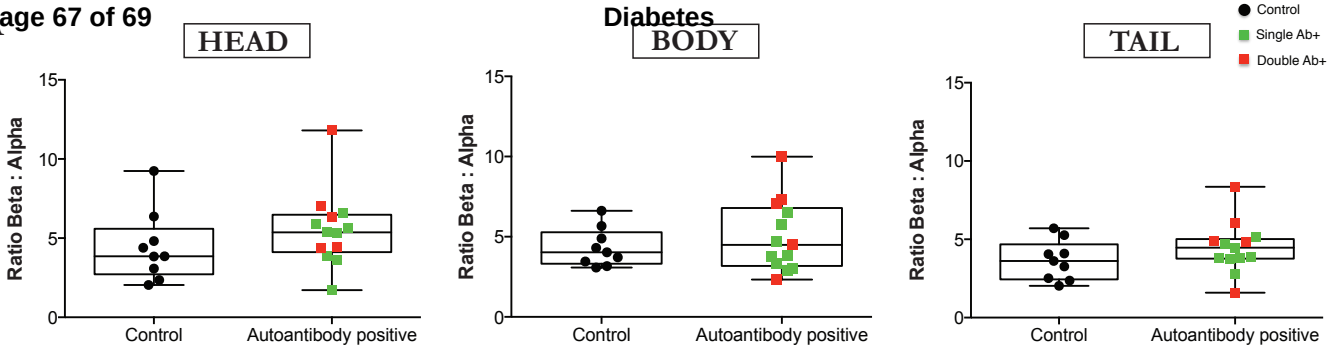

B

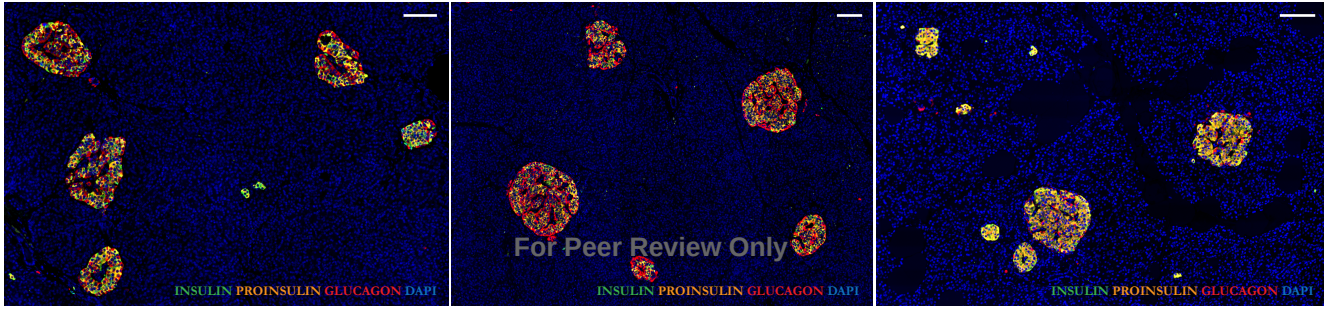

Table S1 shows extended demographic and histological information, and pancreatic regions analyzed.

nPOD ID	Donor Type	Gender	Age	BMI	Duration	C-Peptide	Time ICU	HLA	Regions analyzed	Autoantibodies	Histopathology by nPOD
6044	Autoab Pos	Male	41.4	27.4	-	13.55	-	A*01:01/33:01 B*14:02/37:01 C*06:02/08:02 DRB1*01:02/15:01 DQA1*01:01/01:02 DQB1*05:01/06:02 DPA1*01:03/01:03	Head, Body, Tail	GADA+	Ins+/Gluc+ islets, normal sizes and distribution. Ki67 normal
6080	Autoab Pos	Female	69.2	21,3	-	1.84	1	A*02:01/11:01 B*35:01/44:02 C*04:01/05:01 DRB1*01:01/04:01 DQA1*01:01/03:01 DQB1*03:01/05:01 DPA1*01:03/01:03 DPB1*04:01/04:02	Head, Body, Tail	GADA+ mIAA+	Ins+/Gluc+ normal islets. No islet infiltrates. Chronic pancreatitis, mild, multifocal, mixed
6123	Autoab Pos	Female	23.2	17.6	-	2.01	4	A*02:01/24:02 B*35:01/51:01 C*01:02/03:03 DRB1*08:01/11:01 DQA1*04:01/05:01 DQB1*03:01/04:02 DPA1*01:03/01:03 DPB1*04:01/04:01	Head, Body, Tail	GADA+	Ins+ islets, various sizes. Low Ki67
6147	Autoab Pos	Female	23.8	32.9	-	3.19	3	A*02:01/02:01 B*08:01/15:01 C*03:04/07:01 DRB1*03:01/04:01 DQA1*03:01/04:01 DQB1*03:01/04:02 DPA1*01:03/02:01 DPB1*01:01/02:01	Head, Body, Tail	GADA+	Ins+/Gluc+ normal islets. No infiltrates
6154	Autoab Pos	Female	48.5	24.5	-	<0.05	4	A*02:01/03:01 B*07:02/07:02 C*07:02/07:02 DRB1*09:01/15:01 DQA1*01:02/03:01 DQB1*03:03/06:03 DPA1*01:03/01:03 DPB1*02:01/04:01	Head, Body, Tail	GADA+	Ins+ (very weak)/Gluc+ islets, plentiful. Very mild, multifocal CD3+ infiltrates acinar regions and interstitial. Moderate fatty infiltrates acinar regions
6158	Autoab Pos	Male	40.3	29.7	-	0.51	3	A*03:01/24:02 B*15:01/49:01 C*03:04/07:01 DRB1*04:01/13:02 DQA1*01:02/03:01 DQB1*03:01/06:04 DPA1*01:03/01:04 DPB1*04:01:15:01	Head, Body, Tail	GADA+ mIAA+	Ins+/Gluc+. Exocrine atrophy, mild. Focal mild chronic pancreatitis
6167	Autoab Pos	Male	37	26.3	-	5.43	3	A*01:01 , 03:01 DRB1*04:04 , 15:02 DQA1*01:03 , 03:01 DQB1*03:02 , 06:01	Head, Body, Tail	IA-2A+ ZnT8A+	Ins+/Gluc+ islets, normal. No infiltrates. Mild acinar fat. Low Ki67 except for focally high in acinar and ducts
6170	Autoab Pos	Female	34.4	36.9	-	4.29	7	A*29:02 , 74:01 DRB1*04:01 , 13:03 DQA1*02:01 , 03:01 DQB1*02:02 , 03:01	Head, Body, Tail	GADA+	Ins+/Gluc+ islets. Slight acinar atrophy and fatty replacement. No infiltrates other than 1 foci of chronic pancreatitis
6181	Autoab Pos	Male	31.9	21.9	-	0.06	2	A*03:01 , 11:01 DRB1*01:01 , 04:01 DQA1*01:01 , 03:01 DQB1*03:02 , 05:01	Head, Body, Tail	GADA+	Ins+/Gluc+ islets, normal. No infiltrates
6184	Autoab Pos	Female	47.6	27	-	3.42	6	A*02:06 , 68:03 DRB1*04:07 , 04:07 DQA1*03:01 , 03:01 DQB1*03:02 , 03:02	Head, Body, Tail	GADA+	Ins+/Gluc+ islets, normal numbers and morphology. Very mild CD3 infiltrate in acinar region. Mild acinar Ki67. Mild fatty replacement. Mild ductal sludge
6197	Autoab Pos	Male	22	28.2	-	17.48	3	A*02:02 , 24:02 DRB1*03:02 , 07:01 DQA1*02:01 , 04:01 DQB1*02:02 , 04:02	Head, Body, Tail	GADA+ IA-2A+	Ins+/Gluc+ islets, plentiful. Insulitis (rare). Islet hyperemia. Mild, multifocal chronic pancreatitis. Low Ki67
6267	Autoab Pos	Female	23	23.5	-	16.59	4	A*01:01, 11:01 DRB1*04:01, 04:04 DQA1*03:01, 03:01 DQB1*03:02, 03:02	Head, Body, Tail	GADA+ IA-2A+	Ins+/Gluc+islets in normal numbers and density. Insulitis found in all regions. Islets appear well demarcated with some having fibrosis. Mild CD3+ infiltrates acinar region with mild exocrine atrophy
6310	Autoab Pos	Female	28	23.9	-	10.54		A*03:01, 30:01 DRB1*07:01, 11:02 DQA1*02:01, 05:01 DQB1*02:02, 03:19	Head, Body, Tail	GADA+	Ins+/Gluc+ islets, numerous, some hyperplastic and >500um. Islet nuclear pleomorphism- mild. Insulitis- low grade, periphery and foci. Pseudoatrophic islets observed and other islets with low beta to alpha ratio. Multifocal, mild exocrine CD3+ infiltrates. Multifocal, mild chronic interstitial fibrosis
6029	No diabetes	Female	24	22.6	-	-	-	A*03:01/31:02 B*15:15/35:01 C*01:02/04:01 DRB1*04:03/08:02 DQA1*03:01/04:01 DQB1*03:02/04:02 DPA1*01:03/01:03 DPB1*04:02/51:01	Head, Body, Tail	Negative	Ins+/Gluc+ normal islets. Mild fatty infiltrate. Low Ki67. Endothelium in islets fairly prominent

nPOD ID	Donor Type	Gender	Age	BMI	Duration	C-Peptide	Time ICU	HLA	Regions analyzed	Autoantibodies	Histopathology by nPOD
6073	No diabetes	Male	19.2	36	-	0.69	3	-	Head, Body, Tail	Negative	Ins+/Gluc+ islets; mild, multifocal parenchymal mixed infiltrate. Endocrine staining intensity weaker than normal
6091	No diabetes	Male	27.1	35.6	-	7.71	-	A*01:01/25:01 B*18:01/39:06 C*07:02/12:03 DRB1*08:01/15:01 DQA1*01:02/04:01 DQB1*04:02/06:02 DPA1*01:03/01:03 DPB1*02:01/03:01	Head, Body, Tail	Negative	Ins+/Gluc+ normal islets, many large especially in head and body. Degree of fatty infiltrate moderate. No infiltrates identified
6102	No diabetes	Female	45.1	35.1	-	0.55	2	A*03:01/31:01 B*08:01/44:02 C*05:01/07:01 DRB1*03:01/04:01 DQA1*03:01/05:01 DQB1*02:01/03:01 DPA1*01:03/02:01 DPB1*01:01/02:01	Head, Body, Tail	Negative	Ins+/Gluc+ islets. Multifocal, mild periductal and peri-islet fibrosis. Mild CD3+ acinar regions. Low Ki67. Moderate fatty replacement exocrine tissue. Chronic pancreatitis- mild, multifocal
6104	No diabetes	Male	41	20.5	-	20.55	3	A*29:02/68:01 B*39:06/44:03 C*12:03/16:01 DRB1*07:01/13:01 DQA1*01:01/02:01 DQB1*02:01/05:01 DPA1*01:03/02:02 DPB1*01:01/03:01	Head, Body, Tail	Negative	Ins+/Gluc+ islets. Mild adipose infiltration exocrine regions
6165	No diabetes	Female	45.8	25	-	4.45	5	A*01:01, 02:01 DRB1*13:01, 15:01 DQA1*01:02, 01:03 DQB1*06:02, 06:03	Head, Body, Tail	Negative	Ins+/Gluc+ numerous islets, normal sizes. No infiltrates. Mild acinar fat
6168	No diabetes	Male	51	25.2	-	-	7	A*02:01, 24:02 DRB1* 01:03, 04:04 DQA1*01:01, 03:01 DQB1*03:02, 05:01	Head, Body, Tail	Negative	Ins+/Gluc+ islets, all sizes. Normal density. Low Ki67. Variable fatty infiltrates acinar regions
6251	No diabetes	Female	33	29.5	-	1.92	4	A*02:01, 24:02 DRB1*04:01, 11:01 DQA1*03:01, 05:01 DQB1*03:01, 03:01	Head, Body, Tail	Negative	Ins+/Gluc+ islets, numerous, including single cells. No significant lesions
6271	No diabetes	Male	17	24.4	-	11.47	0.5	A*02:01, 02:06 DRB1*07:01, 15:02 DQA1*01:01, 02:01 DQB1*02:02, 05:01	Head, Body, Tail	Negative	Ins+/Gluc+ islets, numerous, medium sized
DiViD 1	T1D	Female	25	21	4 (weeks)	-	-	A *01:01, 02:01 B*08:01, 40:01 DRB1*01:03, 03:01 DQB1*05:01, 02:01	Tail	IA-2A+ ZnT8A+GADA+ mIAA+	Ins+/Gluc+ islets. Only a few insulin containing islets left. Some of them with insulitis.
DiViD 2	T1D	Male	24	20.9	3 (weeks)	-	-	A*02:01, 11:01 B*18:01, 40:01 DRB1* 04:01, 13:01 DQB1*03:02, 06:03	Tail	IA-2A+ ZnT8A+GADA+	Ins+/Gluc+ islets. Only a few insulin containing islets left. Altered islet morphology.
DiViD 3	T1D	Female	34	23.7	9 (weeks)	-	-	A*01:01, 24:02 B*08:01, 15:01 DRB1*03:01, 04:01 DQB1*02:01, 03:02	Tail	IA-2A+ ZnT8A+GADA+	Ins+/Gluc+ islets. Moderate amount of insulin containing islets left. High infiltration in some insulin deficient islets. Insulitis.
DiViD 4	T1D	Male	31	25.6	5 (weeks)	-	-	A*02:01 B*15:01, 35:01 DRB1*04:01 DQB1*03:02	Tail	IA-2A+GADA+ mIAA+	Ins+/Gluc+ islets. Only a few insulin containing islets left.
DiViD 5	T1D	Female	24	28.6	5 (weeks)	-	-	A*02:01, 03:01, B*18:01, 40:01 DRB1*03:01, 04:01 DQB1*02:01, 03:02	Tail	IA-2A+GADA+ mIAA+	Ins+/Gluc+ islets. Only a few insulin containing islets left.
DiViD 6	T1D	Male	35	26.7	5 (weeks)	-	-	A*01:01, 29:02 B*08:01, 44:03 DRB1*03:01, 07:01 DQB1*02:01, 02:02	Tail	GADA+	Ins+/Gluc+ islets. Most of the islets still contain insulin.
6362	T1D	Male	24.9	28.5	0	0.38		A*03:01, 11:01 DRB1*01:03, 03:01 DQA1*01:01, 05:01 DQB1*02:01, 05:01	Tail	GADA+	Ins+/Gluc+ islets, moderate reduction numbers of Ins+ islets. Many islets with abnormal morphologies (large, fusing smaller islets, irregular outlines, fibrosis). Insulitis in most Ins+ islets and small number of Ins- islets. Islet nuclear pleomorphism with variable hydropic degeneration. Generally low islet Ki67+ but occasional islet with high Ki67+ in non-beta cells. Moderate to high acinar Ki67+ cells. Mild to moderate acinar CD3+ infiltrates and variable fatty infiltration. Moderate exocrine atrophy with variable intralobular fibrosis.

Table S1: Extended donor information. Autoab Pos, autoantibody positive donor. T1D, type 1 diabetic donor. Age and duration of disease are expressed in years unless otherwise indicated; BMI, body mass index; C-peptide is expressed in ng/ml; time ICU, time spent in the Intensive Care Unit; ZnT8A, zinc transporter 8 autoantibodies; IA-2A, intracytoplasmic domain of the tyrosine phosphatase IA-2 autoantibodies; mIAA, micro assay for insulin autoantibodies; GADA, glutamic acid decarboxylase 65 autoantibodies. – indicates not determined or not available.